Osservatorio Astronomico di Cagliari	Ital-FLAMES	Osservatorio Astronomico di Palermo

VERY LARGE TELESCOPE

FLAMES-UVES
Data Reduction Software
Design and Architecture Report

Document Issue: **2.1**

Document Number: **VLT-TRE-ITA-13750-0002**

Date of Issue: **November 13, 2000**

Prepared by:	Approved by:	Released By:
G. Mulas **F. Damiani** **I. Porceddu** **P. Caldara**	**G. Mulas**	**C. Cacciari**

Contents

1 Introduction

1.1 Scope

This document establishes the specifications for the design and architecture of the Data Reduction Software (DRS) of the 'fibre' mode of the **UVES** (Ultraviolet-Visual Echelle Spectrograph) instrument used in connection to the optical fibre positioner **FLAMES** mounted on VLT Kueyen (UT2) telescope. The **UVES** spectrograph is mounted on the Nasmyth B Platform of VLT Kueyen and is fed in its fibre mode by up to 8 independent fibres.

1.2 Document overview

Chapter 1 states the purpose and organisation of the document.

Chapter 2 collects all the references, the acronyms and conventions used throughout the document .

Chapter 3 describes the assumptions underlying the whole DRS design, including instrumental characteristics, and the specifications which the DRS will have.

Chapter 4 outlines the application of the standard and optimal extraction algorithms to the specific problem of adjacent, partially overlapping cross dispersed spectra, the required extensions and the respective advantages and drawbacks.

Chapter 5 describes, from a conceptual point of view, the operative steps which compose the data reduction.

Chapter 6 outlines, in the schematic form of tables, the actual steps of the data reduction, how they will be implemented and the flow of data between them.

Chapter 7 describes in some detail the modules which will compose the DRS, specifying where they are used in the data reduction, as some of them are used, unchanged, in different places of the data reduction chain, on different inputs and producing different outputs.

Chapter 8 describes some numerical tests that have been performed to assess the feasibility of the algorithms and their dependence on the assumptions (in terms of instrumental stability).

2 Documentation

2.1 Related documents

The following documents constitute part of this document. In the event of conflict between the documents referenced here and the content of this document, the content of the present document supersedes all previous documentation.

2.2 Applicable documents

The following documents are to be considered as part of this document. They describe the work to be carried out and the constraints to be taken into account:

[**AD 1**] Ital-FLAMES Project Management Plan, Issue 1, VLT-PLA-ITA-13750-0001

[**AD 2**] UVES User Manual, VLT-MAN-ESO-13200-1825

[**AD 3**] FLAMES Operation and Calibration Plan, Issue 1.0, VLT-PLA-ESO-13700-1788

[**AD 4**] UVES Pipeline and Quality Control User's Manual, Issue 1.1, VLT-MAN-ESO-19500-1619

[**AD 5**] Annex to FLAMES/UVES DRS Design and Architecture Report, Issue 1.0, VLT-TRE-ITA-13750-0002 (annex)

[**AD 6**] Meeting of the ITAL-FLAMES Consortium Minutes, Issue 1.0, VLT-MIN-ITA-13750-0004

[**AD 7**] GIRAFFE Spectrograph and Fibre Subsystems: Technical Specification, Issue 1.1, VLT-SPE-ESO-13730-1657

[**AD 8**] FLAMES Templates Reference Guide, Issue 1.0, VLT-SPE-ESO-13700-1995

[**AD 9**] Data Flow for VLT instruments Requirement Specification, Issue 1.0, VLT-SPE-ESO-19000-1618

[**AD 10**] ESO-MIDAS User Guide, Volume A: System, MIDAS Release 98NOV, MID-MAN-ESO-11000-0002

[**AD 11**] ESO-MIDAS User Guide, Volume B: Data reduction, MIDAS Release 98NOV, MID-MAN-ESO-11000-0003

[**AD 12**] FLAMES UVES Requirements on the UVES software for the Fibre Mode of UVES, Issue 1.0, VLT-SPE-ESO- 13200-2100

2.3 Reference documents

The following documents are to be considered as useful documents to be used for referencing purposes.

[**RD 1**] Hill, V., 'GIRAFFE, UVES: Spectra separation and contamination', Informal ESO report 1999

[**RD 2**] Zaggia, S., Informal ESO report (2000) on spectra separation and contamination in UVES fibre mode

[**RD 3**] Horne, K., 'An optimal extraction algorithm for CCD spectroscopy', 1986, PASP, 98, 609

[**RD 4**] Robertson, J.G., 'Optimal extraction of single-object spectra from observations with two-dimensional detectors', 1986, PASP, 98, 1220

[**RD 5**] Mukai, K., 'Optimal extraction of cross dispersed spectra', 1989, PASP, 102, 183

2.4 Acronyms

As follows you can find all the acronyms used in this document.

DRS Data Reduction Software
ESO European Southern Observatory
FF Flat Field of all the fibres
FLAMES Fibre Large Array Multi Element Spectrograph
RON Read Out Noise
SF Science Frame
SNR Signal to Noise Ratio
TBC To Be Confirmed
TBD To Be Defined
UVES UV Echelle Spectrograph
VLT Very Large Telescope
WF Wavelength Frame (calibration frame)

2.5 Conventions

As follows you can find all the conventions (both the typographic and the naming ones) used in this document.

2.5.1 Naming Conventions

FF$_{even}$ Flat Field with the even fibres
FF$_{n}$ Flat Field with the n-th fibre
FF$_{odd}$ Flat Field with the odd fibres
[**calibrations**] Frame made during the calibration time
[**database**] Frame contained in the **UVES** database
[**outx.y**] Output from the stage x.y of the procedure

2.5.1.1 Naming Conventions for schemes

bpM bad pixel Mask
CCT Cross-Correlation table
DB Dark and Bias Frames
FFa Flat Field with all fibres
FFo Flat Field with odd fibres
FFe Flat Field with even fibres
IFSFF Full Slit Flat Field
IOT Inter-Order table
IF Illumination Fraction
OFS Order-fibre polynomial Solution
OFT 1st guess order finding table
SF Science Frame
SFF Single fibre Flat Field
SS Science Spectrum
TC Throughput Correction
WCS Wavelength Calibration (1st guess) solution
WS Wavelength Spectrum
WF Th-Ar Frame

2.5.2 Typographic conventions

$S(i,j)$ Science frame matrix
$F_n(i,j)$ n-th fibre Flat Field matrix

$V(i,j)$ Variance matrix
$M(i,j)$ Mask matrix
parameter Parameter to be used in procedure
[parameter] Optional parameter
`Name.tbl` Filename of a MIDAS table
`NamePO.bdf` Filename of a MIDAS frame in pixel-order space
`NamePP.bdf` Filename of a MIDAS frame in pixel-pixel space

3 Requirements and specifications

In this chapter we outline the basic requirements that the data reduction software (DRS) for **UVES** in **FLAMES** mode will satisfy. The DRS method and detailed implementation are described in subsequent chapters. Here, we also outline those instrument characteristics that are most relevant for the DRS development, as they are known at the time of release of this document.

3.1 Data reduction software requisites

Through the development of the DRS design, we have taken care that it satisfies a number of different requirements. Among the most important are:

- Accuracy: The DRS has to be able to retrieve a reduced spectrum that is as similar as possible to the 'original' input spectrum of the light falling into the telescope. To this aim, we have tried to identify all sources of errors (e.g. noise and systematic errors), and handle them in such a way as to minimise their impact to the end result.
- Extraction of maximum information content: the software has to be as such as to extract in the most through way the information content of the acquired data. To this aim, emphasis will be put throughout this document on the need for very accurate calibration data.
- Reliability in automatic mode: once integrated in a pipeline (under **ESO** responsibility), the DRS must be able to run without human intervention. Should deviant cases occur (e.g. numerical instabilities, mismatches between flat-fields and data, unreasonably bad fits) various quality controls will be made available to the user, allowing him/her to judge if the final reduction products are of a quality adequate to his/her scientific aims.
- Fast execution speed: within its options, the DRS will contain at least one method capable to perform a quick reduction (as reliably as possible) in near real time at the telescope. This will allow the observer to decide if the exposure just taken fulfils his/her science requirements, timely enough to allow him/her to take an additional/different **UVES** exposure.
- Ease of use: the DRS is designed to be simple to use, even by the astronomer with no specific experience on **UVES** or **FLAMES**. Therefore, only a few free parameters will be determined by the user, and default values for them will be provided.

3.2 FLAMES-UVES characteristics

The **FLAMES-UVES** characteristics constitute the basic assumptions (and constraints) on which the DRS will be developed, and their details are therefore of vital importance for our work.

The **FLAMES-UVES** characteristics most relevant to our purposes are the following:

- Only a subset of **UVES** Instrument Settings will be available in **FLAMES** mode, namely (see the document AD 6):
  - 3 Standard Wavelength Configurations (red arm of UVES):
    - cross disperser 3 with central wavelength 520 nm;
    - cross disperser 3 with central wavelength 580 nm;
    - cross disperser 4 with central wavelength 860 nm;
  - 1 Standard Detector Binning (1×1, TBD), no nonstandard binnings.
- The detector of the red arm of **UVES** is a mosaic of two CCDs, of size 2048×4096 pixels each. Between the two CCDs there is a gap of width approximately equal to one spectral order.
- Each raw frame output from **UVES** will contain $n \sim 35$ echelle orders (including both CCDs); each order will contain up to $n_f = 8$ separate spectra (but likely $n_f = 6$ in the blue setups), produced by the n_f fibres. In ordinary mode all of these fibres will come in from the **FLAMES** positioner, but a simultaneous calibration mode is also offered, in which one of the fibres will be fed by a separate calibration unit. The total number of fibres being used at the same time, and more generally the frame format, is the same both in ordinary and in simultaneous calibration mode. The total number of spectra present on a single frame (2 CCDs) will therefore be $n_f \times n$, where the exact values of n and n_f will depend on the specific setup being used.
- Thanks to effective light scrambling along the fibres, the cross-dispersion PSF can be safely assumed to be the same for flat-field frames and science frames to less than 1% (see the document AD 6).
- During the **FDR** meeting, Andreas Kaufer reported that the stability of **UVES** in the direction perpendicular to dispersion is presently a couple of pixels at best. This depends on variations of the cross-disperser turntable positions due to:
  - temperature variations of **UVES** (to be characterised by ESO and, if at all possible, corrected in software)
  - the discrete step of the encoder controlling the cross-disperser turntable angle corresponds to 0.3 pixels on the detector, and it keeps jittering back and forth seeking the optimal position.

  This jittering will possibly blur a science exposure ($\sim 30'$) in the direction perpendicular to dispersion. On the other hand, calibration exposures will be always very much shorter ($< 2'$), and jittering will be assumed to be negligible for them. In any case, the effect of such small variations of the cross-disperser turntable positions will be very accurately given by a simple, rigid shift in the direction perpendicular to dispersion of the distribution of light on the detector.

- Again during the **FDR** meeting, Andreas Kaufer stated that FF exposures with the same setup used during the night will be taken with **UVES** in slit mode and be available during the data reduction. The slit length will be large enough for the exposed part of the FF frame to cover all the fibres to be used, including a couple of extra pixels to allow for drift and jitter.

A set of datasets obtained with test fibres have been made available, in order to estimate the actual performance of **UVES** in fibre mode. The analysis of these test datasets has shown that:

- **UVES** spectral lines are straight, namely perfectly aligned with CCD columns. Any misalignment/curvature amounts to only a fraction of a pixel over the entire slit width, and is about one order of magnitude smaller across a fibre, in fibre mode. This width is a tiny fraction of the intrinsic line width, and therefore needs *not* to be taken into consideration any further, i.e. we will always consider that spectral lines run strictly parallel to CCD columns. Doing otherwise would merely make procedures more complicated, with a substantially increased error propagation, surely larger than any nominally increased accuracy of the method, that as seen can be only very marginal. While wavelength can be safely assumed to depend only on the CCD column *within a fibre*, a wavelength shift can occur between different fibres. This will be taken into account in the DRS.
- Different spectral orders are well separated, with totally negligible cross-contamination, but in the bluer part of the spectrum (five bluest orders) a contamination between extreme fibres of adjacent orders is increasingly present.
- Fibres belonging to the same spectral order are so close together that some contamination between adjacent fibres definitely occurs, at the level of a few percent. Inter-fibre cross-contamination, therefore, cannot be considered negligible in the data reduction strategy. The level of contamination as measured from test data can be assumed as an upper limit to the final value, since the diameter of final fibres will be slightly smaller.
- One spurious order diffracted by the cross-disperser is present, superimposed on the useful data, in the setup centred around 860 nm. The DRS will try to minimise its impact on the reduction procedure, as far as possible, but the user will have to be warned in advance that some wavelength regions will be affected by a systematic error, limiting the achievable S/N ratio.
- The fibre bundles coming from the two plates of **FLAMES** enter **UVES** one on each side of the entrance slit. Their centres are separated by about 400 μm from each other, and therefore by about 200 μm from the centre of the **UVES** entrance slit. Despite this, FF frames taken with **UVES** in slit mode can be used to adequately correct for the pixel to pixel variations and, for the reddest setup, for ripples due to interference fringes.
- The normalised cross-dispersion light distribution, for any given fibre and order, varies very slowly in the dispersion direction and can be considered constant over ranges of a few tens of pixels.
- For all the setups of **UVES** to be used, the slope of the orders in pixel-pixel space lies between $\sim$0.034 and $\sim$0.039. The centre of a given order will therefore move by 1 pixel in the direction perpendicular to dispersion if one moves along the order in the dispersion direction by 25$\sim$30 pixels.

4 Data reduction method

4.1 Standard versus optimal extraction

In order to obtain one-dimensional (1-D) spectra (intensity vs. wavelength) from two-dimensional (2-D) data arrays (as is the case with a CCD), a method must be used that integrates the raw spectral data along the spatial (cross-dispersion) direction. Two methods are commonly used to do this task: 'standard' extraction and 'optimal' extraction.

Standard extraction prescribes that a fixed-width window has to be chosen encompassing all (or most) of the spectrum across the spatial direction, and the values of all pixels comprised within this window are summed to yield the object spectrum at the corresponding wavelength. All considered pixels receive the same weight, except for 'partial' pixels at the window upper/lower borders. The 2-D image has to be previously prepared by subtracting from it the bias, dark current, and diffuse scattered light components, by removing/flagging CCD defects, by removing cosmic-ray spots, and by flat-fielding to compensate for pixel-to-pixel detector non-uniformities and/or ripples due to various spurious interference patterns. There does not exist a unique rule for prescribing extraction limits, and the user is usually left with a relative freedom to vary them. The sky contribution to the extracted spectrum has to be determined in a similar way, and subtracted from the object spectrum as a subsequent step. In general, a considerable amount of user (interactive) intervention is needed for a complete spectral reduction.

Optimal extraction was initially developed by Horne (RD 3) and Robertson (RD 4), with the explicit purpose of minimising the variance of the extracted spectra, especially in the case of spectral data with a low signal-to-noise ratio (SNR). It therefore fulfils the two requirements of extracting most thoroughly the information contained in the raw data, and that of maximum accuracy in general (including low-SNR data). The theoretical maximum gain in low-SNR spectra, with respect to standard extraction, is about 40% more SNR, that amounts to a gain in effective exposure time of 70% (RD 3). In other words, if a weak spectrum is extracted with optimal extraction, its SNR will be the same of a spectrum extracted with standard extraction *but exposed 70% longer*. The raw data must be prepared for optimal extraction in the same way as for standard extraction, except that cosmic rays are not removed beforehand, but in the course of the extraction procedure; in turn, this allows the removal of weaker cosmic-ray hits. While not requiring a fixed spatial window width, optimal extraction requires the knowledge of the spatial, cross-dispersion profile of the 2-D spectrum on the CCD, as well as an accurate evaluation of pixels variances. Once these data are known, optimal extraction proceeds practically independent from user intervention, and is therefore well suited for an automated procedure. In optimal extraction, the raw data pixels corresponding to a given wavelength are linearly combined along the spatial direction using weight factors, instead of being simply summed. Weights are chosen in such a way as to minimise the variance of the sum, on the basis of the known cross-dispersion profile. As shown by Horne (RD 3), the resulting linear combination of pixels is exactly the same as when one is fitting the model cross-dispersion profile to the pixel data.

The price that optimal extraction has to pay with respect to standard extraction is a slight increase in computational time, that has to be evaluated in each specific case; we however do not expect that this can be a serious drawback with present-day computer speeds. The user has always the option to use standard extraction. The standard method would yield, in most cases, inferior results to optimal extraction, and therefore the latter will be the default. One exception is that of calibrations poorly matched to the data: in this case, one of the basic assumptions of the optimal extraction algorithm fails, namely knowledge of the spatial, cross-dispersion profile of the 2-D spectrum on the CCD. We include an algorithm capable to compensate for small, rigid drifts and (in part) jitters in the direction perpendicular to dispersion, but this will still fail for different kinds of mismatch. On the other hand, the standard extraction algorithm is, to some extent, less sensitive to a mismatch between calibrations and science data, and can thus be used as a backup solution.

4.2 Slit mode versus fibre mode

One important thing to take into account in the case of **FLAMES-UVES** is that the light enters the spectrograph through optical fibres rather than through a slit placed in the focal plane. This implies advantages as well as drawbacks.

A fibre collects all of the light falling within its size on the focal plane. If the seeing disk happens to be smaller than the fibre (sky-projected) size, the fibre will collect all of the object light (for a point-like object). If the seeing disk happens to be larger than the fibre size, the fibre will collect only part of the object light, leading to photometric inaccuracy. This may render the **FLAMES-UVES** spectrograph unsuitable for spectrophotometric purposes in general. In any case, the fibre will also always collect some sky contribution.

Because of the large number of internal reflections within a fibre across its length, the light carried by a fibre will be strongly scrambled, and its output light will therefore have a cross-fibre profile almost independent from the light spatial profile at fibre entrance. Therefore, the cross-fibre output light profile will be the same regardless of current observing conditions, and therefore it will be *highly reproducible*. A very small difference in the cross-fibre output light profile between science data (i. e. sources on the sky) and calibration data (i. e. calibration lamps) may be brought about by the different geometries of the incoming light beams. However, any differences between these profiles can be safely assumed to be below 1% (see the document AD 6).

This is unlike conventional ‘slit mode’ observing, where the current seeing directly affects the cross-dispersion profile width. One advantage of ‘slit mode’ is instead the usual availability of a sky spectrum on either side of the object spectrum. In fibre mode, on the contrary, the sky spectrum cannot be disentangled from the object spectrum by examining the output of a single fibre, and its measurement requires instead one (or more) separate fibres.

Another distinctive peculiarity of a fibre spectrograph such as **FLAMES-UVES** is that *all* light that enters the spectrograph passes through the fibres, *including the flat-field calibration data taken in fibre mode.* For the reasons outlined above, therefore, the flat-field (FF) image will be characterised by a light distribution profile along the cross-dispersion direction "*identical*" to that of the object spectra, fibre by fibre for each order. However, as mentioned in section 3.2, science exposures may suffer from significant drift and jitter of the cross-disperser turntable position. Since to each cross-disperser turntable position corresponds a rigid displacement of the light distribution profile along the cross-dispersion direction, with the assumptions made in section 3.2 the following properties apply:

1. the cross-dispersion light distribution in a given science frame is the result of a convolution between the cross-dispersion light distribution in the FF calibration frame taken in fibre mode and the distribution of rigid shifts in the direction perpendicular to dispersion corresponding to the history of drifts and jitters during the science exposure;
2. a small (~1 pixel) rigid shift in the direction perpendicular to dispersion of a flat-field calibration frame taken in fibre can, for a given order, be accurately obtained by applying a corresponding shift in the dispersion direction, applying suitable normalisation coefficients. In this way, if only integer shifts in the dispersion direction are used, shifts in the perpendicular direction can be obtained with an accuracy of ~0.039 pixels.

These requirements are yet to be confirmed, as the impact of a mismatch between FF frames and science frames on the accuracy of the data reduction procedures will depend on the shape of the cross-dispersion light distribution and on the cross-talk between adjacent fibres *in the final setup.* The above figures were derived from numerical simulations with profiles and fibre separations similar to those in **FLAMES-UVES** test data (Section 8). To date, it is still TBD whether such strict stability requirements in the cross-dispersion direction will be met by **UVES** (see section 3.2 and document AD 12).

In what follows, we will take for granted that **FLAMES-UVES** FF images will match very closely (within the limits defined above) in every detail the spatial distribution of detected signal on the CCD, that will be measured for actual objects in the sky. This property of FF differs from the usual case, where the FF spatial profile is substantially smoother (flatter) than the object spatial profile; in this latter case, the FF is meant to reflect mainly the pixel-to-pixel sensitivity variations across the CCD chip and spurious interference fringes, if present. In our case, we have a more complex situation:

- we have *two* different kinds of FF images, namely FF images taken with **UVES** in slit mode and FF images taken with **UVES** in fibre mode;
- more components are to be identified in the FF images, some showing up in both kinds of FF images, some only in the ones in fibre mode:
    1. as before, a high-spatial-frequency pixel-to-pixel sensitivity variation component (both slit and fibre mode);

2. a mid-frequency component describing the fibre cross-dispersion profile (only fibre mode)
3. another mid-frequency component, evident in the setup centred around 860 nm and mostly negligible in the others, due to spurious interference fringes (both slit and fibre mode);
4. a low-frequency component describing longer-scale effects such as blaze function, possible vignetting, etc. (both slit and fibre mode);
5. a component describing the difference in throughput among different fibres (only fibre mode).

We will assume throughout that FF images will have a SNR per pixel so high that any pixel-to-pixel variation in the FF image actually reflect a true sensitivity variation. Also, combining the object data with the FF has to introduce the least possible error in the calculation, which can be done only if the FF has negligible relative error in any pixel.

In the **FLAMES-UVES** system, the fibres are placed at short distances from one another on the **UVES** entrance slit, and it turns out that their light distributions partially overlap. The importance of this effect has still to be quantitatively assessed in a definitive way for the final fibres, but has been estimated to be of the order of *a few* percent if the fluxes fed into the adjacent fibres are similar. Thus, in the case of two low-SNR spectra recorded in two adjacent fibres this small cross-contamination may not constitute a problem. It indeed does, instead, if two high-SNR spectra are being recorded in adjacent fibres, and even worse if the two fibres contain one a high-SNR spectrum and the other a much weaker one. In this latter case, the relative contamination of the weaker spectrum by the stronger one may even reach or exceed 100%. Therefore, the DRS will include a method to deconvolve partially cross-contaminated spectra to recover the 'true' individual spectra.

4.3 Reduction strategies

Using available calibration data, especially flat-field frames, it would be of advantage to perform a pre-processing of calibration frames before the start of science observations. Such a pre-processing would include e.g. the definition of spectral orders, and the modelling of light distribution on the FF images (as explained in the next sections), thus sparing potentially a considerable amount of processing time during the night.

4.3.1 Optimal extraction

For optimal extraction the observed data will be fitted with a model, derived using FF data matching closely the science exposure.

Preliminary steps to light-distribution fitting are:

- subtraction of bias and dark current images;
- selection of the illuminated regions on the image, order by order;

- construction of a (logical) mask containing flags for dead/hot pixels or other bad CCD features;
- fitting of diffuse/scattered light in non-illuminated regions, and its subtraction from the whole image;
- division of the resulting image by the (preliminary bias-subtracted) slit mode FF frame;
- construction of a 'variance image' for the image hereby obtained, including propagated contributions from all above steps.

Once these steps are completed, a model must be individuated that describes the light distribution as imaged by the CCD detector. Such a model must include, for each order and at each position along the dispersion coordinate, a factor describing the variation of illumination along the cross-dispersion direction, times a factor describing the larger-scale illumination pattern on the CCD, times a factor describing the throughput of individual fibres (pixel-to-pixel sensitivity variations are cancelled after division by the slit-mode flat field).

From the discussion in section 4.2 it turns out that such a model is closely related to the flat-field image itself. In fact, as a first approximation the FF image describes where fibres belonging to a given order are located, their widths and profiles, and their long-range behaviour and fibre throughput. This approach is a rather "direct" one, and therefore preferable to an empirical/analytical model based on the FF image itself. If the UVES instrument were strictly stable (no thermal/pressure drifts, no jitter during long exposures) the correspondence between FF and science frames would be an exact one, and the FF images would provide an extremely detailed of the illumination pattern in the science frames. Since drifts and jitters are however present, to a non-negligible extent, we cannot use such a straightforward approach, of using the FF illumination pattern "as is" to describe that in the science frame, but we must transform the available FF frames to reproduce, or "mimic", as closely as possible, the light distribution in the science frames. The actual inaccuracies, propagated through the data reduction procedure, arising from a mismatch between FF and science data, as estimated from **UVES** test data taken with experimental fibres, are described in section 8. The simulations and tests described in that section also allow us to know how accurate our FF "reconstruction" has to be, in order to produce good and reliable end results.

Actually, since as described in section 4.2 we have to fit a (partial) superposition of independent fibres, the model we are going to fit to the data cannot be a single profile given by the reconstructed FF image at the given order location and wavelength pixel. Instead, we need one FF image per each fibre, to be obtained from a set of FF frames unaffected by cross-fibre contamination (see section 4.4). We will indicate the FF image relative to fibre n as FF_n (the FF image for fibre n, but divided by the slit-mode FF will be indicated as FF'_n, while the reconstructed FF image for fibre n will be indicated as FF''_n).

As explained in more detail in section 5.5, to reconstruct the FF''_n flat-fields from the input FF'_n flat-fields, we need to know the (time-integrated) distribution of drifts that have occurred during the science exposure. One robust method to derive this drift distribution from the science data itself is to compute a correlation function between the science frame and the input FF' frames, one order at a time. In doing so, we take advantage of the small slope of the light distribution for each order, as imaged by the CCD. Under these circumstances, even a very small shift across dispersion (e.g. 0.05 pix) may be mimicked by a shift by an integer number of pixels along dispersion. Therefore, we compute a correlation function by shifting the input FF' relative to the science image along dispersion, and integrating over one whole order, and the resulting correlation function will peak at the (average) drift between input FF' and science frame. If a substantial jitter is also present during the science exposure, it will also be reflected in a broadening of the same correlation function. We eventually obtain the reconstructed FF''_n frames by shifting the input FF'_n frames by a suitable number of pixels along dispersion, as dictated by the correlation function peak (order by order). If a non-negligible jitter is also present, we will use instead a linear combination of shifted FF'_n frames to get the desired single-fibre FF''_n frames.

For each order and wavelength pixel, therefore, we will fit the data with a linear combination of the eight functions FF''_n. The parameters to be fit are only the normalisation constants of these eight functions, and each normalisation constant is the sought spectral intensity at the given wavelength pixel. The problem therefore is simply to perform an eight-parameter linear fit, involving a step of matrix inversion that can be straightforwardly solved using standard techniques (e. g. Gauss-Jordan elimination). In this way the deconvolution of the contamination between adjacent fibres is automatically made: were it not for this effect, we would not have to do one eight-parameter linear fit, but eight one-parameter linear fits, independently from one another. The eight-parameter fit reflects therefore that we are actually taking into account the cross-contamination between fibres.

For each order and wavelength pixel, the profile fitting will be iterated, each time rejecting only the pixel that deviates most from the model, only if its deviation exceeds a specified number of times the standard deviation of that pixel (standard sigma-clipping). Such a threshold will have to be carefully selected on the basis of the expected stability with which the cross-dispersion light profile given by the FF image matches that of science frames. In very high S/N science exposures, even a very slight mismatch, too small to have a significant impact on the quality of the resulting data, may produce a deviation of a few standard deviations in good pixels. The threshold for rejection must be accordingly tuned *not* to reject such pixels. The threshold will be taken from a MIDAS keyword whose default value will be decided at commissioning time, based on real data.

After each rejection, the expected pixel variances are recomputed on the basis of the best-fit model (rather than directly from the data, Horne RD 3). The fit is then repeated, a further rejection is made, and so on until no more pixels are rejected. This allows to remove cosmic rays that pollute the observed data. This step is crucially sensitive to mismatches between the FF and science frame, which may cause a large number of spurious pixel rejections and a wrong estimate (and elimination) of the cross-fibre contamination.

Once this step is done, we will have for each order and wavelength pixel a set of eight spectral intensity parameters, that constitute directly the spectra we are searching for, with all corrections applied.

There is one possible exception to this: depending on their placement on the focal plane, and on the position of the guide star chosen, some of the fibres may be partially vignetted. Moreover, fibre throughputs are slightly dependent on flexures, so that their ratios may be somewhat different from those derived (and corrected for) from FF frames in the afternoon. These effects will be essentially wavelength independent, and will therefore translate in a different attenuation factor for each fibre in that exposure. This will obviously result in photometric inaccuracy. If an accuracy better than 2% in relative fluxes is required, Nasmyth screen calibrations will need to be used (see the definition of templates in document AD 8).

The last step to be done is wavelength calibration. Wavelength calibration frames will be reduced in the same way as object fibres, in order to obtain a separate wavelength calibration spectrum for each fibre. Each of these spectra will then follow a pretty conventional route to obtain a separate wavelength dispersion relation for each fibre. This part will be made as automatic as possible, taking advantage of the small number of offered instrument setups and its stability. We will adapt the existing **UVES** context with a minimum of modifications.

Since no sky subtraction is possible with the given setup, as discussed in section 4.2, if needed it should be done *post facto*, namely devoting some fibre(s) to sky measurement, reducing it in the same way as object fibres, and subtracting the sky spectrum from the object spectra at the very end, *after wavelength calibration*. Unless different fibres are vignetted in different ways on the focal plane, since the extracted spectra are already corrected for different fibre throughput, the sky spectrum can be simply subtracted "as it is" from the object spectra. If, instead, there is indeed differential vignetting, a relative correction factor will have to be estimated. This is straightforward to obtain automatically if a matching Nasmyth screen calibration frame has been taken. Otherwise it will have to be estimated off-line with human intervention, by iteratively matching the intensity of sky emission lines. This relative correction factor might be used to restore, to some extent, the photometric accuracy of attenuated fibres (TBC at commissioning time).

4.3.2 Standard extraction

In contrast to optimal extraction, standard extraction is conceptually simpler, may be more robust (no fit has to converge), but is in principle less accurate for low-SNR spectra. Preliminary steps to it are:

1. subtraction of bias, dark current images;
2. the definition of the regions (in the FF frames) occupied by each fibre for each order (not just the region for each order);
3. removal (flagging) of cosmic-ray hits from the science frame, that unlike optimal extraction cannot be done during extraction itself;
4. construction of a (logical) mask containing flags for dead/hot pixels or other bad CCD features;
5. fitting of diffuse/scattered light in non-illuminated regions, and its subtraction from the whole image.
6. division of the resulting image by the (preliminary bias-subtracted) slit mode FF frame;

Steps 1, 4, 5 and 6 are common to both standard and optimal extraction, while steps 2 and 3 are peculiar to standard extraction. Step 3 must be performed either by the standard technique of stacking multiple exposures or by some sort of ad-hoc filtering (TBD).

A cross-dispersion window width w has to be chosen, that will determine the region used for extraction, for each position along the dispersion direction. A default (and maximum) value for w will be the inter-fibre separation itself, but the user will be allowed to use a smaller w if he/she wants. Pixels flagged as defects or cosmic rays will be included neither in the extraction of the spectra, nor in the extraction of the flat-field, so that this effect cancels out in the final, flat-fielded reduced spectra. Depending on the value of w, there will be a more or less pronounced cross-fibre contamination, that the algorithm has to deconvolve. The amount of contamination is derived by applying the same extraction to the single-fibre flat-field frames FF''_n, and examining the 'cross-fibre' terms with respect to 'diagonal' terms. As in optimal extraction, a linear system of equations has to be therefore inverted in order to derive the 'true' contribution to each wavelength pixel for each fibre. Unlike optimal extraction, however, this is not part of a fitting process, and the user has no automatic feedback (quality control) on the good functioning of the procedure. For the same reason, there are no iterations, but a single-step calculation. We should remark that standard extraction may be inaccurate in such cases as the presence of low-level cosmic ray events, that may have escaped the preliminary cleaning, or bad detector pixels not known in advance of reduction. We also remark that our standard extraction (*which includes fibre deconvolution*) has to compensate drift and jitter in the science exposure *just as the optimal extraction*, to produce accurate results. In particular, drift and jitter have two separate effects:

- The drift produces an average shift in the cross-dispersion direction between the FF_n and the science frame to be reduced. This, if uncorrected, would have the effect of centring the integration windows in the wrong place. The simplest way to correct this is to estimate this cross-dispersion displacement, apply the appropriate offset to the integration windows on the science frame, compute an appropriately "shifted" FF_n and use the latter to reduce the science frame.
- The jitter "blurs" the cross-dispersion PSF on the science frames with respect to that in the FF_n, thereby increasing the inter-fibre contamination accordingly. This, if uncorrected, leads to an inadequate subtraction of the contamination fraction from the spectra of neighbouring fibres. To correct this, on must estimate the jitter in the science frame, compute an appropriately shifted *and* "blurred" FF''_n and use the latter to reduce the science frame.

The only advantage of the standard extraction is that it can be made less sensitive to jitter reducing the integration window w: in this way one discards the parts of the frame in which there is a larger inter-fibre contamination, hence reducing the impact of wrongly correcting it, at the expense of a considerable loss of signal. During the reduction, the fraction of light that is discarded due to the choice of a small w is estimated, as well as its impact on the S/N ratio. Moreover, it must also be kept in mind that the choice of a w substantially smaller than the cross-dispersion profile of a fibre may result in ripples caused by the discrete pixelisation; for them to cancel out with those resulting from the extraction of the FF image, the cross-dispersion PSF in the science frame must accurately match that of the "adjusted" FF_n used to reduce it. While accurately estimating the average drift in a science frame is relatively trivial, the capability of the DRS to accurately estimate the jitter, and hence its effectivity at compensating for it, will depend on the actual typical jitter patterns in **UVES**. This will have to be assessed on real data taken with the instrument in its final configuration. Once the actual impact on the quality of the extracted spectra of the mismatch between science and calibration frames will be known, it will be possible to decide if and when re-calibration should be recommended.

Eventually, wavelength calibration and sky subtraction are done, with no difference with respect to the 'optimal' case.

4.4 Required calibration data

According to **ESO** specifications, the calibration sequence will be carried out during instrument setup (in the afternoon) and not ordinarily during the night.

Special requirements that may directly increase the amount of time required to assemble all needed calibration data will have therefore no impact on observing efficiency during night time, and therefore do not constitute a serious drawback.

The following frames will be used by the DRS, in addition to the science frame (SF) to be reduced:

- flat field frames taken both in slit and fibre mode (FF);
- wavelength calibration frames (WF);
- bias and dark current frames.

All of these calibration frames will be taken in repeated exposures, in a sufficient number to allow removal of cosmic ray hits (using the usual stacking/median filtering techniques), and to obtain, at least for FF frames, a very high SNR, whose importance has been stressed in section 4.2. In the following we will assume that bias and dark current frames will have been subtracted as a very starting step from all other frames, namely image data, FF and wavelength calibration frames. As a second preliminary step on image data, FF and wavelength calibration frames, scattered light will be estimated from the inter-order regions and subtracted. As a third preliminary step, all frames taken in fibre mode will be divided by the FF frame taken in slit mode. This step will effectively remove pixel to pixel sensitivity variations and spurious interference fringes. As a consequence, the parts of the frames which are not adequately illuminated in the FF image in slit mode will not be used in the subsequent reduction.

As explained in section 4.3.1, the FF data needed for our spectral reduction procedure is not a single frame per data image (or per night), but rather a set of 8 single-fibre FF frames. Since cross-contamination occurs only between adjacent fibres, a single-fibre FF may be extracted from a FF in which only *odd-numbered* or *even-numbered* fibres are illuminated. Thus we define $FF_{odd} = FF_1 + FF_3 + FF_5 + FF_7$, and $FF_{even} = FF_2 + FF_4 + FF_6 + FF_8$. In this way, for a most complete and accurate data reduction, we need two FF frames (FF_{odd} and FF_{even}) instead of one. It is important that FF_{odd} and FF_{even} be taken both with the same exposure time and calibration lamp flux, with an accuracy possibly much higher (but at very least no worse) than that of the best science frames. As the stability of the calibration lamp is likely not good enough for this purpose, a third set of FF frames in which *all* the fibres are illuminated at the same time will be needed in order to accurately determine the relative throughput of adjacent fibres. If an accuracy of better than $\sim$2% in the calibration of relative throughputs is required by the user, a Nasmyth screen calibration can be used to replace this latter FF frame.

To each image (and its FF frame) a logical mask (M) will be associated, of the same size, which will be used to select pixels to be used in the subsequent processing (good pixels), while flagging/rejecting bad CCD pixels not to be included in the calculations. For each image we will also compute a corresponding frame (V), containing the estimated variances for each pixel, that is strictly necessary for optimal extraction (section 4.1). This variance image is computed on the basis of the image data itself, and of the knowledge of the read-out noise of the CCD and its gain (conversion factor between ADUs and electrons).

The standard deviation will be propagated through every subsequent calculation.

4.5 Problems and backup solutions

As is evident from all previous discussion, the whole procedure just described is crucially dependent on a very precise match between the light distribution in the "adjusted" FF''_n image(s) and that in the object spectral image. This depends on the precision with which drift and jitter in each science frame can be evaluated. Although we do provide a scheme to accomplish this, it might be not precise enough for a reduction scheme aimed at the most complete recovery of the scientific information. In particular, as will be seen in more detail later, while the determination of the drift is relatively straightforward, accurate and reliable, the determination of the jitter pattern can be more troublesome. While jitters smaller than $\sim$0.3 pixels, even if uncorrected, seem to lead to a mild, probably acceptable degradation of the quality of the extracted spectra (see numerical tests in section 8), for some purposes this might still be a problem. First, the existence of a problem has to be detected, therefore quality controls (**QC**) are provided, and a warning will be issued to the user immediately. Second, a decision must be taken on how to proceed in such a case, either by the user in off-line mode or by the **ESO** pipeline/DFS in online mode.

As a check of the good functioning of the procedure described in section 4.3.1, we may straightforwardly take a goodness-of-fit indicator such as χ^2, whose value should be recorded for each order and wavelength pixel. If persistently bad fits (with overall χ^2 larger than an assigned threshold) are encountered throughout the whole spectral image, a warning will be issued by the DRS. The χ^2 value will be output anyway, to be checked by the user or the pipeline (**QC #1**).

Alternatively, the fit may be successful, but in order to be so it may require to discard an exceedingly large number of pixels (say, more than 50%, or another suitably chosen threshold), that cannot uniquely be due to cosmic rays or detector defects, but rather to a non-negligible mismatch between FF and spectral image data. Even in this case a warning will be issued. The fraction of rejected pixels will be output, to be checked by the user or the pipeline (**QC #2**).

As far as remedies are concerned, the standard extraction method will be used, correcting only the average drift and using a reduced integration window w in order to minimise the impact of cross-contamination in the resulting spectra, with all the shortcomings outlined in section 4.3.2.

5 Data reduction procedure

Schematically, the optimal extraction procedure will run through the steps listed below (and see also Figure 5.1):

1. Bias and dark current subtraction from SF and FF;
2. definition of the order/inter-order regions on the fibre mode FF frames (regions occupied by each order and regions between them);
3. fit of scattered light in inter-order regions and a few pixels in the bluest orders where there is no inter-order spacing, and its subtraction from FF and SF;
4. division of all fibre mode frames by slit mode FF;
5. estimation of drift and jitter in the SF;
6. if necessary, repeat step 3, taking into account the drift derived above and also consequently repeat steps 4 and 5;
7. build “synthetic” single-fibre FF''_n that mimic the drift and jitter measured in the SF;
8. optimal extraction of Science and Thorium/Argon spectra with σ-clipping, revised variances, and iterations (as described in sections 4.1 and 4.3.1);
9. determination of the dispersion relations from Thorium/Argon spectra in pixel-order space, as obtained from the preceding step;
10. rebinning of the extracted object spectra from pixel space to wavelength space;
11. sky spectrum subtraction from finally reduced object spectra (if requested by the user);
12. order merging.

These steps are described in detail in the following sections. Step 1 is obvious and will not be described further.

Steps 1, 4, 9, 10, 11 and 12 can be performed with existing MIDAS procedures; the fact that the instrument is fibre-fed has either no effect on them (1, 4) or simply implies that the same, unchanged procedure will have to be repeatedly and separately applied to spectra belonging to different fibres (9, 10, 11 and 12). Step 2 will be performed with a modified version of the DEFINE/HOUGH procedure, whose algorithm was seen to work well in simulated data, but has to made aware of the presence of multiple fibres within each order. Steps 3, 5, 6, 7 and 8 will be performed by procedures to be written ad hoc for **UVES** in **FLAMES** mode.

The standard extraction will instead comprise the following steps:

1. Bias and dark current subtraction from SF and FF;
2. definition of the order/inter-order regions on the fibre mode FF frames (regions occupied by each order and regions between them);
3. cosmic-ray detection and flagging in the SF;
4. fit of scattered light in inter-order regions, and its subtraction from FF and SF;
5. division of all fibre mode frames by slit mode FF;
6. estimation of drift and jitter in the SF;
7. if necessary, repeat step 4, taking into account the drift derived above and also consequently repeat steps 5 and 6;
8. build “synthetic” single-fibre FFs that mimic the drift and jitter detected in the SF;
9. standard extraction of Science and Thorium Argon spectra with fibre deconvolution;
10. determination of the dispersion relations from Thorium/Argon spectra in pixel-order space, as obtained from the preceding steps;
11. rebinning of the extracted object spectra from pixel space to wavelength space;
12. sky spectrum subtraction from finally reduced object spectra (if requested by the user);
13. order merging.

Steps 1, 3, 4, 5, 11, 12 and 13 can be performed with existing MIDAS procedures; the fact that the instrument is fibre-fed has either no effect on them (1, 3, 4, 5), or implies that the same, unchanged procedure will have to be repeatedly and separately applied to spectra belonging to different fibres (10, 11, 12 and 13). Step 2 will be performed with a modified version of the DEFINE/HOUGH procedure, whose algorithm was seen to work well in simulated data, but has to made aware of the presence of multiple fibres within each order. Steps 6, 7, 8 and 9 will be performed by procedures to be written ad hoc for **UVES** in fibre mode.

An operation mode with simultaneous wavelength calibration is offered for high precision radial velocity measurements, whereby the last fibre always carries a wavelength calibration spectrum. Since the

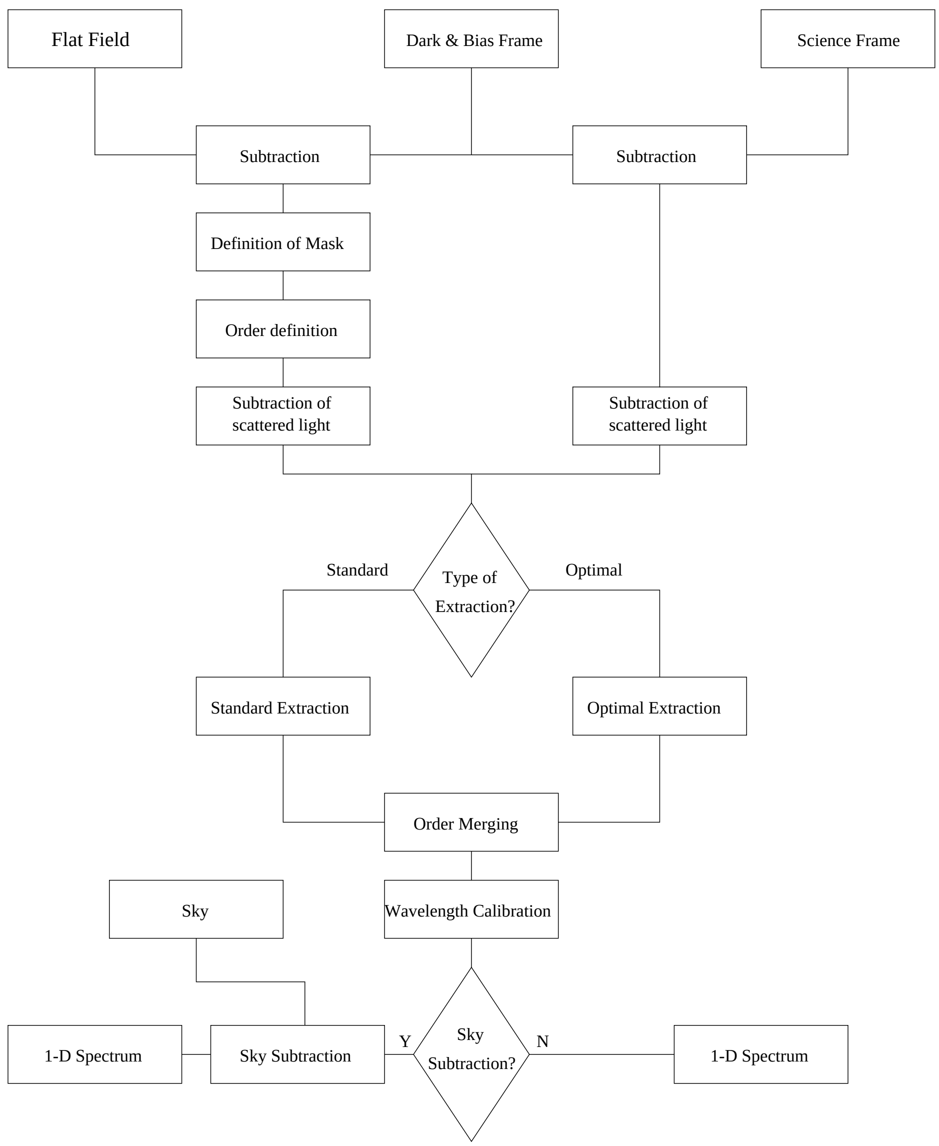

Figure 5.1: Block diagram of the overall reduction strategy

format of the frame is unchanged in this operation mode with respect to the “ordinary” mode, the reduction will largely follow the same steps in both operation modes. The spectra can and will be extracted exactly in the same way regardless to what is fed into each fibre. By and large, the only difference is that one of the extracted spectra is a wavelength calibration spectrum from the calibration unit. This wavelength calibration spectrum, taken simultaneously with the astronomical observations, will be used, before rebinning, to derive a higher order correction for the wavelength calibration derived from the spectra taken with the wavelength calibration lamp of the **FLAMES** fibre positioner. This higher order correction can be derived in different ways, and applied at different stages of the data reduction, and there is no single, well defined and generally accepted way to do it. In particular, some users may want to apply the higher order correction at the stage of rebinning to wavelength space (e.g. as a correction to the dispersion relation), and will therefore want to work on the extracted spectra *before* rebinning. The **DRS**, for this observing mode, will implement one way to derive and apply this higher order correction.

The optimal extraction procedure for science frames taken with in the simultaneous calibration observing mode will run through the following steps:

1. Bias and dark current subtraction from SF and FF;
2. definition of the order/inter-order regions on the fibre mode FF frames (regions occupied by each order and regions between them);
3. fit of scattered light in inter-order regions and a few pixels in the bluest orders where there is no inter-order spacing, and its subtraction from FF and SF;
4. division of all fibre mode frames by slit mode FF;
5. estimation of drift and jitter in the SF;
6. if necessary, repeat step 3, taking into account the drift derived above and also consequently repeat steps 4 and 5;
7. build "synthetic" single-fibre FFs that mimic the drift and jitter detected in the SF;
8. optimal extraction of Science and Thorium/Argon spectra with σ-clipping, revised variances, and iterations (as described in sections 4.1 and 4.3.1);
9. determination of the dispersion relations from all Thorium/Argon spectra in pixel-order space, as extracted from both the wavelength calibration frame in which the fibres are fed with the calibration unit of the positioner and from the simultaneous calibration fibre;
10. evaluation of the difference between the dispersion relation derived from the simultaneous calibration fibre on the SF and the one derived from the simultaneous calibration fibre on the frame with the Th/Ar lamp on all fibres; this difference is applied, as a correction, to the dispersion relations of all other fibres;
11. rebinning of the extracted object spectra from pixel space to wavelength space;
12. sky spectrum subtraction from finally reduced object spectra (if requested by the user);
13. order merging.

Steps 1, 4, 9, 11, 12 and 13 can be performed with existing MIDAS procedures; the fact that the instrument is fibre-fed has either no effect on them (1, 4) or simply implies that the same, unchanged procedure will have to be repeatedly and separately applied to spectra belonging to different fibres (9, 11, 12 and 13). Step 2 will be performed with a modified version of the DEFINE/HOUGH procedure, whose algorithm was seen to work well in simulated data, but has to made aware of the presence of multiple fibres within each order. Steps 3, 5, 6, 7, 8 and 10 will be performed by procedures to be written ad hoc for **UVES** in **FLAMES** mode.

The standard extraction procedure for science frames taken with in the simultaneous calibration observing mode will run through the following steps:

1. Bias and dark current subtraction from SF and FF;
2. definition of the order/inter-order regions on the fibre mode FF frames (regions occupied by each order and regions between them);
3. cosmic-ray detection and flagging in the SF;
4. fit of scattered light in inter-order regions, and its subtraction from FF and SF;
5. division of all fibre mode frames by slit mode FF;
6. estimation of drift and jitter in the SF;
7. if necessary, repeat step 4, taking into account the drift derived above and also consequently repeat steps 5 and 6;
8. build “synthetic” single-fibre FFs that mimic the drift and jitter detected in the SF;
9. standard extraction of Science and Thorium Argon spectra with fibre deconvolution;
10. determination of the dispersion relations from all Thorium/Argon spectra in pixel-order space, as extracted from both the wavelength calibration frame in which the fibres are fed with the calibration unit of the positioner and from the simultaneous calibration fibre;
11. evaluation of the difference between the dispersion relation derived from the simultaneous calibration fibre on the SF and the one derived from the simultaneous calibration fibre on the frame with the Th/Ar lamp on all fibres; this difference is applied, as a correction, to the dispersion relations of all other fibres;
12. determination of the dispersion relations from Thorium/Argon spectra in pixel-order space, as obtained from the preceding steps;
13. rebinning of the extracted object spectra from pixel space to wavelength space;
14. sky spectrum subtraction from finally reduced object spectra (if requested by the user);
15. order merging.

Steps 1, 3, 4, 5, 12, 13, 14 and 15 can be performed with existing MIDAS procedures; the fact that the instrument is fibre-fed has either no effect on them (1, 3, 4, 5), or implies that the same, unchanged procedure will have to be repeatedly and separately applied to spectra belonging to different fibres (10, 12, 13 and 14). Step 2 will be performed with a modified version of the DEFINE/HOUGH procedure, whose algorithm was seen to work well in simulated data, but has to made aware of the presence of multiple fibres within each order. Steps 6, 7, 8, 9 and 11 will be performed by procedures to be written ad hoc for **UVES** in fibre mode.

5.1 Order definition

This step is most conveniently done in the afternoon, just after calibration data are taken, and before any night science observation.

In this and the following sections we will deal with images made of pixels arrays $I(i,j)$, with $i = 1,...N$ being the row index (varying along the y axis) and $j = 1,...M$ the column index (varying along the x axis). The dispersion direction runs at a small angle to the x axis, and therefore the j index also indicates the wavelength pixel. Within the same spectral order, indicated with m, all pixels with the same j index share all the same wavelength. At a given column j, a spectral order m is identified by its lower and upper limits, namely two row numbers that we indicate as i_{low} and i_{upp}.

The identification of the different spectral orders on the spectral image frame is the first non-trivial task to be performed. This is best done using the available FF frames taken in fibre mode. An existing MIDAS task such as the DEFINE/HOUGH, made for non-fibre echelle spectrographs, is already able to accurately trace the all the fibres and orders present in such a FF frame; however, as it is it does not recognise which fibres belong to which order. Therefore, a suitably modified version of DEFINE/HOUGH will be used.

We assume to have available the two FF frames FF_{odd} and FF_{even} (defined in section 4.4). On each of them, fibre images are well separated, and well defined across the whole image because of the high SNR, requested for all FF images. On both of these frames, the first steps of DEFINE/HOUGH are independently performed, namely:

- a rough approximation of the scattered background light is performed by heavy filtering, and subtracted;
- the Hough transform of each resulting frame is performed, and from it a first approximation of the slope and intercept of all fibres present in all orders is derived;
- for each of the fibres detected in the hough transforms the maxima are found and followed, building a table containing a list of coordinates of pixels tracing each detected fibre.

At this point, a new procedure is inserted, which makes use of the approximate order definition previously derived from the FORMAT/UVES procedure to label the lists of points in the table according to fibre number and order number. The coordinates of the pixels in the table thus obtained are then fitted with a bivariate polynomial with fixed offsets between fibres belonging to the same order. All derived fit coefficients are stored in a second array C. We thus derived the fibre positions for each order. The knowledge of fibre positions is also used to extract from the frames FF_{odd} and FF_{even} the individual-fibre FF frames, FF_n.

The boundaries i_{low}, i_{upp} of each order m for each j are therefore the location of fibre #1, *minus a suitable quantity* Δi, and the location of the last fibre, *plus* Δi. The quantity Δi must be chosen large enough to include the wings of the light distribution of the fibres, but small enough not to include light coming from neighbouring orders. Its final value will be fixed from the analysis of the fibre-fed **UVES** commissioning data.

Between the image regions occupied by the various orders, just identified, there will remain regions where the only measured signal is due to diffuse, scattered light within the spectrograph. The definition of order boundaries, therefore, implies also a definition of the (complementary) regions where the scattered light contribution has to be extracted. In order to have a better sampling of these latter regions, the quantity Δi just defined should be kept as small as possible, still within the constraints already stated.

As a last step, two more boundaries $i_{low}^{slit}, i_{upp}^{slit}$ (distinct from the ones defined above) of each order m for each j need to be derived, defining the parts of the detector illuminated in the slit mode FF frames. For each column and order, the median of the $\sim$30 (to be tuned) pixels around the centre of the order is calculated, a threshold set at about half the obtained value and the well illuminated region around the centre of the order above the latter threshold is thus selected. In the actual spectral extraction, only this selected region of all frames will be used.

As a conclusion, at the end of this stage we will have completely identified all regions in the FF frames where the individual spectral orders are found, fibre by fibre, as well as the region between the various orders where only scattered light is supposed to be present.

5.2 Subtraction of scattered light

All pixels (or a uniformly-spaced subset) in the inter-order regions are fitted with a bivariate polynomial of second/third order in i and j, meant to reproduce the slowly-varying scattered light contribution. This is done both on science frame and fibre mode FF, separately, and the model fit is then subtracted from the respective images. The fit in itself is linear in all parameters, and presents no special difficulties at all. However, **UVES** data in **FLAMES** mode will have no inter-order space in the bluest orders. This results in two problems:

1. A cross-dispersion drift of a couple of pixels between the FF frame and the science frame may cause the wings of the bluest orders to contaminate the selected inter-order space. If one is not very conservative in the choice of the inter-order positions, this results in a systematic overestimate of the background; on the other hand, if one is conservative in the choice of the inter-order positions, there will be no usable inter-order space in a large part of the frames, in which the background cannot be sampled in the conventional way. Since the drift is actually estimated later, the workaround is to fit the background two times: first before drift estimation, then (if necessary) again, using the actual inter-order space, taking into account the estimated drift and hence avoiding systematic contamination.

2. Anyway, even with a two pass approach as described above, a conventional background fitting can be performed only on the available inter-order space (i. e. none in the bluest orders) and then must be extrapolated.

Alternatively, a more complex background fitting method has to be used, which has to simultaneously fit both the background and the spectra in selected locations in the bluest orders. Such an extended background fit is only possible and will only be provided for optimal extraction.

5.3 Division by slit mode Flat Field frame

All the frames taken in fibre mode are, at this stage, divided by the slit mode Flat Field frame. The new flat field frames thus obtained will be henceforth indicated as F'_n.

5.4 Single fibre F'_n construction and cleaning

The frames F'_n obtained with the division of the single fibre F_n by the slit mode Flat Field frame FF_{slit} reflect, apart from a normalisation factor $\mathrm{N}_n(j,m)$, only the cross-dispersion PSF, since the pixel to pixel sensitivity variations and (if present) spurious interference fringes have been divided away. We may thus write:

$$\mathrm{F}'_n(i,j) = \mathrm{N}_n(j,m)\mathrm{PSF}_n(i,j,m). \tag{5.1}$$

For a given order m and fibre n, the *shape* of the PSF is assumed to vary very slowly with j, while its centre of gravity is a known function, which can be locally represented as a straight line and has a small slope $s(m) \equiv di/dj$ ($<$0.039), essentially dependent only on m and only very weakly on j. Therefore, if we want to mimic a small shift in the cross-dispersion direction, of order $\delta i \sim 0.1$ pixels, in the F'_n, we may get a very good approximation in the following way:

$$\mathrm{F}'_n(i,j,\delta i) \simeq \mathrm{N}_n(j,m)\mathrm{PSF}_n(i,j+\delta j,m), \tag{5.2}$$

with $\delta j \simeq \frac{\delta i}{s(m)}$.

As a first use of equation 5.2 we note that, for $\delta j = \pm\frac{1}{s(m)}$ we have $\delta i = \pm 1$, resulting in

$$\mathrm{F}'_n(i\pm 1,j) \simeq \mathrm{N}_n(j,m)\mathrm{PSF}_n(i,j\pm\frac{1}{s(m)},m), \tag{5.3}$$

and this will be used to fill the holes in F'_n due to bad pixels: missing/bad values will be replaced by the ones taken at a properly shifted i and j, according to equation 5.3.

5.5 Determination of drift and jitter in the science frame

As explained in section 3.2, the instability in the cross-disperser position results in rigid shifts of the illumination pattern on the detector in the direction perpendicular to dispersion. Therefore, the illumination pattern is not simply proportional to the single fibre flat field frames, but instead is proportional to a *convolution* of the latter with a function $g(\delta i)$ reflecting the history of drift and jitter during the given science frame. Of course, $g(\delta i)$ will generally be different for every science frame.

As outlined in section 4.3.1, the basic shape of the drift/jitter function $g(\delta i)$ can be derived from a study of the correlation function between the science frame and the FF' frame (sum of single-fibre FF'_n, provided that there is no drift between FF_{odd} and FF_{even}, or that this drift has been already corrected for). Taking advantage of the non-zero slope $s(m)$, we may relate a shift δi with a shift δj, and write

$$g(\delta i) = g(s(m)\delta j) = g'(\delta j) \tag{5.4}$$

Since a shift $\delta i \sim 0.05$ pix across dispersion corresponds roughly to a shift $\delta j \sim 1$ pix along dispersion, and this latter is easily applicable, it is clear that the function $g'(\delta j)$ is much more easily computed than $g(\delta i)$. To compute $g'(\delta j)$, we first note that the correlation function reaches a maximum value for a shift along j (dispersion direction) such that the science frame resembles most closely the shifted FF frame, while has a minimum value when science frame and shifted FF are out of phase (fibre centers in the science frame coincide with inter-fibre minima in the FF). In formulae, defining the correlation function for order m as $C_m(\delta j)$, and the domain occupied by order m as A_m:

$$C_m(\delta j) = \sum_{i,j \in A_m} \sum_n \mathrm{F}'_n(i,j,\delta j)\mathrm{S}(i,j) \tag{5.5}$$

(here, S(i,j) is the science frame). The function $C_m(\delta j)$ is computed using a large number of pixels, and is in general very accurately known; therefore, the location of its maximum is very well defined, yielding an average drift δj_0 (and a corresponding cross-dispersion drift $\delta i_0 = s(m)\delta j_0$), where the drift distribution $g'(\delta j)$ will peak. As a first approximation for $g'(\delta j)$ we take therefore a simple Dirac delta function $\delta(\delta j - \delta j_0)$. As a further step, the drift distribution around its average value δi_0 gives rise to a broadening of the maximum of the correlation function $C_m(\delta j)$, and one may try to deconvolve this broadening to obtain the detailed shape of $g'(\delta j)$. However, for a distribution $g(\delta i)$ not wider than 0.6-1.0 pixels (across dispersion), this broadening is very small, and its deconvolution may be diffcult. Moreover, tests using detailed simulations, described in section 8 show that a broadening of this amount in δi does not affect appreciably the extraction procedure (even optimal extraction that is most sensible to mismatches). Therefore, for the purpose of our reduction procedure, representing $g(\delta i)$ as a delta function centered on δi_0 is enough, as long as the jitter during one exposure does not exceed an amplitude of 0.6-1.0 pixels (across dispersion). If commissioning data will show that these limits are exceeded, a slightly refined (tabular) representation for $g(\delta i)$ may become necessary, including non-zero contributions at shifts δj in a neighborhood of δj_0.

5.6 Construction of the illumination model

In order to extract the spectra for a science frame, we have to construct a "synthetic" single fibre flat field frame sharing the same convolution with $g'(\delta j)$, i. e.

$$\mathrm{F}''_n(i,j) = \int \mathrm{F}'_n(i,j,\delta j) g'(\delta j) d(\delta j), \tag{5.6}$$

where $\mathrm{F}'_n(i,j,\delta j)$ is calculated according to equation 5.2. This integral is evaluated by a discrete sum over a grid with the same resolution of the tabular representation of $g'(\delta j)$ derived in the preceding section.

5.7 Single spectra extraction with fibre deconvolution

5.7.1 Optimal extraction

After having selected the region occupied by each order m on the FF and science frame, we then perform the spectrum extraction proper, using an optimal extraction method, for all eight fibres simultaneously. Since wavelength is strictly constant along a column j (for a given order m and fibre n), spectral extraction is done independently for each column j. The problem is therefore decoupled in a series of separate extractions, one for each value of j and m. Optimal extraction then amounts to fit the cross-dispersion profile of the science frame, $S(i,j)$, with a linear superposition of "adjusted" single-fibre flat-field profiles, $\mathrm{F}''_n(i,j)$. The fit is made for a fixed j, and $i \in [i_{low}, i_{upp}]$ (i_{low} and i_{upp} are dependent on j and m). The value of the χ^2 statistics is:

$$\chi^2 = \sum_{i=i_{low}}^{i_{upp}} M(i,j) \frac{(S(i,j) - \sum_{n=1}^{8} c_n F''_n(i,j))^2}{V(i,j)}. \tag{5.7}$$

Here, $M(i,j)$ is the mask frame, whose value is 1 for accepted pixels, and 0 for pixels to be excluded from the computation (e.g. bad pixels). $V(i,j)$ is the variance image, namely an array whose pixels contain the computed variances of the science frame pixels and FF frames; the c_n are the normalisation coefficients to be fitted, namely the extracted spectrum for each fibre n (and order m and wavelength pixel j). By minimising χ^2 we get:

$$\frac{\partial \chi^2}{\partial c_k} = 0 = -2 \sum_{i=i_{low}}^{i_{upp}} M(i,j) \frac{S(i,j) - \sum_{n=1}^{8} c_n F''_n(i,j)}{V(i,j)} F''_k(i,j). \tag{5.8}$$

Defining

$$b_k = \sum_{i=i_{low}}^{i_{upp}} M(i,j) \frac{S(i,j) F''_k(i,j)}{V(i,j)} \tag{5.9}$$

and

$$a_{kn} = \sum_{i=i_{low}}^{i_{upp}} M(i,j) \frac{F''_k(i,j) F''_n(i,j)}{V(i,j)}, \tag{5.10}$$

the above equation reduces to the simple linear system

$$\sum_{n=1}^{8} c_n a_{nk} = b_k \tag{5.11}$$

that is easily solved for the unknowns c_n, for each j and m. If it turns out to be numerically convenient, allowing a faster computation, we might use inversion methods specifically suited for tri-diagonal matrices, as is a_{kn} (since $a_{kn} \neq 0$ only if $-1 < k - n < 1$; this is clear from its definition, since non-adjacent fibres have non-overlapping light distributions).

The science frame will undoubtedly also be affected by cosmic ray hits, causing a spuriously large signal in many small spots, each a few pixels across. This strong, localised signal enhancement superimposed on an otherwise smooth cross-fibre profile will cause one or more pixels to deviate badly from the best-fit model profile, locally yielding a large contribution to the total χ^2, say $\chi^2(i)$. For each j,m, the pixel (i,j) having the maximum value of $\chi^2(i)$ is therefore rejected if $\chi^2(i) > \sigma_{clip}^2$, where σ_{clip} is a constant, whose value is chosen by the user (off-line mode) or the **ESO** pipeline (online mode). While $\sigma_{clip} = 5$ is usually a good default value, a choice will have to be based on real commissioning data taken with the instrument in its final configuration. We then set $M(i,j) = 0$ for that pixel, and repeat the fit using the reduced set of pixels. Having done so, we have a best-fit model for the whole science frame. Now the expected variances $V(i,j)$ are recomputed, on the basis of the best-fit model rather than from the data themselves, as it was at the beginning (Horne RD 3). This is iterated until no more pixels are rejected. This completes the extraction of the spectra, for all orders, including fibre deconvolution and correction for different throughputs of the fibres.

5.7.2 Standard extraction

As explained, standard extraction requires an additional preliminary step not needed by optimal extraction: cosmic ray rejection. Cosmic ray rejection may be made using existing routines and we will not deal with it further here.

Once fixed the extraction width w, for each order m and each wavelength pixel j the contribution of a given fibre n will be extracted in an interval of cross-dispersion pixels $[i_{low}(n), i_{upp}(n)]$ (this interval may include 'partial' or 'fractional' pixels), and the extracted spectrum c_n^o will therefore be (for fibre n, wavelength pixel j and order m):

$$c_n^0 = \sum_{i=i_{low}(n)}^{i_{upp}(n)} M(i,j) S(i,j) = \sum_{n'=1}^{8} c_{n'} \sum_{i=i_{low}(n)}^{i_{upp}(n)} M(i,j) F''_{n'}(i,j) \tag{5.12}$$

where the last passage arises by expanding $S(i,j)$ as a sum of contributions of all fibres, weighted by the 'true' spectra c_n. Therefore we may write

$$A(n,n') = \sum_{i=i_{low}(n)}^{i_{upp}(n)} M(i,j) F''_{n'}(i,j) \tag{5.13}$$

and

$$c_n^0 = \sum_{n'=1}^{8} A(n,n') c_{n'}. \tag{5.14}$$

It is therefore clear that we have to invert the matrix $A(n,n')$ (one for each j and m) in order to obtain the true spectra c_n from the observed ones c_n^o. The matrix $A(n,n')$ will be different for different values of w since the limits $(i_{low}(n), i_{upp}(n))$ change with w.

We remark that the resulting spectra are already properly flat-fielded: the $A(n,n')$ matrix contains the single fibre flat fields and the spectra c_n are obtained multiplying the uncorrected c_n^o by the inverse matrix of $A(n,n')$, thereby also dividing them by the appropriate flat field.

5.8 Wavelength calibration

From the instrument specifications listed in section 3.2, it turns out that in **UVES** images spectral lines are perfectly aligned with the CCD columns (y direction). Therefore, for a given order m and fibre n, wavelength depends *only* on the x pixel coordinate. This justifies the optimal extraction procedure as described in the last section, without the need to interpolate between adjacent j pixels to correctly sum only pixels at the same wavelength. The consequence of all this is that wavelength calibration can be done correctly at the end of spectrum extraction proper. At this stage, the spectra are stored in 2D frames in pixel-order space, one frame for each fibre. A separate, independent wavelength calibration will be performed for each fibre. This will just require existing MIDAS **UVES** procedures to loop over fibres.

5.8.1 Simultaneous wavelength calibration

In simultaneous wavelength calibration mode, the last fibre will always carry a Th/Ar spectrum. In particular, this will be present both in the wavelength calibration frame (in which all the other fibres are fed with the Th/Ar lamp on the positioner) and in every given science frame. This will result, for the simultaneous calibration fibre, in a dispersion relation for the wavelength calibration frame and a slightly shifted one for each science frame. Since the dispersion relation is computed as a polynomial, this shift translates simply in a difference in the coefficients of the polynomials. This difference is computed and then applied, as a correction, to the dispersion relations of all the other fibres. These corrected dispersion relations are then used to rebin the science spectra.

5.9 Order merging

The suite of all previous steps will have produced at this point calibrated, one-dimensional spectra that are completely equivalent to those that can be obtained by **UVES** in normal mode, and may therefore be treated using available routines (even those already present in the echelle context of MIDAS), with little or no modification needed.

The spectral sections coming from different fibres but pertaining to the same wavelength range (since there is some wavelength overlap among at least some of the orders) will be averaged at this stage. The average is straightforward since both spectral sections in an overlapping wavelength range have been reduced keeping the correct (relative) normalisation. This is due to the fact that the FF frames used in the course of optimal extraction include of course all long-range effects (such as variations in the blaze function) that make the recorded intensity on the CCD to vary even significantly from one order to the next, especially in the outer regions of the CCD.

5.10 Sky subtraction

If it is deemed important, one of the fibres may be used to record the sky background spectrum, at the user's choice. As the described optimal extraction procedure yields reduced spectra already corrected for differences in throughputs among different fibres, the spectrum extracted from the 'sky' fibre can be plainly subtracted from the object spectra coming from the other fibres, provided that there is no differential attenuation (see section 4.3.1). This operation can be performed at the end of the reduction process.

6 Detailed operative strategies

FLAMES Data Reduction Software will provide a few recipes in order to maximise the information extraction from UVES FLAMES data. The two following tables describe in a synoptic (section 6.1) and an extended (section 6.2 and 6.3) form the schemes, standard and optimal, of the DRS implementation. Short table in section 6.1 also provides a quick look of where the standard and optimal sequences actually differ and where they don't.

The tables' contents take advantage of the UVES environment of MIDAS, as described in the UVES User Guide. Optimal and standard extraction reduction sequences are presented as separate tables, where inputs and outputs are detailed. A short legenda of the used nomenclature includes:

- the keyword “MIDAS” means that an existing MIDAS procedure fulfils our needs,
- “Mod. MIDAS” means that a slightly modified existing MIDAS procedure is used,
- “NEW” means that a brand new procedure has to be implemented in order to deal with that stage of the data flow.
- the origin of each input is indicated in square brackets.
- wherever a science frame or any data structure derived from a science frame is mentioned, it is implicitly intended that a frame or data structure with exactly the same size, containing the estimated variance of each of its pixels, is associated to it, both in input and in output.

6.1 Synoptic view of the DRS implementation

<table>
<tr><th>Stage</th><th>Operation name</th><th>Steps in Standard</th><th>Steps in Optimal</th></tr>
<tr><td>1</td><td>Calibration and Science Frames Preprocessing</td><td colspan="2">• 1.1
• 1.2</td></tr>
<tr><td>2</td><td>Orders Definition</td><td colspan="2">• 2.1
• 2.2</td></tr>
<tr><td rowspan="2">3</td><td rowspan="2">Single fibre Flat Field construction</td><td colspan="2">• 3.1
• 3.2
• 3.3
• 3.4
• 3.5
• 3.6
• 3.7</td></tr>
<tr><td>• 3.8
• 3.9
• 3.10
• 3.11
• 3.12</td><td>• 3.8
• 3.9
• 3.10
• 3.11</td></tr>
</table>

Stage	Operation name	Steps in Standard	Steps in Optimal
4	Spectra extraction	• 4.1 • 4.2 • 4.3 • 4.4 • 4.5 • 4.6 • 4.7 • 4.8	• 4.1 • 4.2 • 4.3 • 4.4 • 4.5 • 4.6
5	Wavelength calibration and rebinning	• 5.1 • 5.2 • 5.3	
6	Sky subtraction	• 6.1	
7	Order Merging	• 7.1	

6.2 Standard extraction

Stage	Input	Operation	Output	Proc.
1.1	• raw Bias frame(s) [calibrations] • raw Dark Current Frame [calibrations] • raw even-fibres Flat Field frame(s) [calibrations] • raw odd-fibres Flat Field frame(s) [calibrations] • raw all-fibres Flat Field frame(s) [calibrations] • raw full slit Flat Field frame(s) [calibrations]	Construction of master Bias, Dark Current and Flat Field frames, cleaned from cosmic ray hits	• (master) Bias frame [out1.1] • (master) Dark Current frame [out1.1] • (cleaned) even-fibres Flat Field frame [out1.1] • (cleaned) odd-fibres Flat Field Frame [out1.1] • (cleaned) all-fibres Flat Field frame [out1.1] • (cleaned) full slit Flat Field frame [out1.1]	MIDAS

Standard extraction

Stage	Input	Operation	Output	Proc.
1.2	• Bias frame [out1.1] • Dark Current frame [out1.1] • raw Science frame [observations] • raw Th-Ar frame [calibrations] • even-fibres Flat Field frame [out1.1] • odd-fibres Flat Field Frame [out1.1] • all-fibres Flat Field frame [out1.1] • full slit Flat Field frame [out1.1]	Subtraction of the bias and dark current values from the Science and calibration frames	• (inter.) Science frame [out1.2] • (inter.) Th-Ar frame [out1.2] • (inter.) even fibres Flat Field frame [out1.2] • (inter.) odd fibres Flat Field Frame [out1.2] • (inter.) all fibres Flat Field frame [out1.2] • (inter.) full slit Flat Field frame [out1.2]	MIDAS
2.1	• single fibre Th-Ar frame [database] • bad pixels Mask [database]	Format check	• 1st guess wavelength calibration solution [out2.1] • 1st guess order finding [out2.1]	**UVES** context
Standard extraction				

Stage	Input	Operation	Output	Proc.
2.2	• even-fibres Flat Field frame [out1.2] • odd-fibres Flat Field frame [out1.2] • bad pixels Mask [database] • 1st guess order finding [out2.1]	Definition of the positions of orders and fibres on the frame	• Order-fibre Table [out2.2] • Inter-order Table [out2.2] • Order-fibre polynomial solution [out2.2]	mod. MIDAS
3.1	• even-fibres Flat Field frame [out1.2] • odd-fibres Flat Field frame [out1.2] • bad pixels Mask [database] • Inter-order table [out2.2]	Computation and subtraction of the scattered light in the even and odd-fibres Flat Field frames, by fitting a low degree polynomial to inter-order positions	• (background subtracted) even-fibres Flat Field frame [out3.1] • (background subtracted) odd-fibres Flat Field frame [out3.1]	MIDAS
3.2	• (inter.) even fibres Flat Field frame [out3.1] • (inter.) odd fibres Flat Field Frame [out3.1] • (inter.) full slit Flat Field frame [out1.2]	Division of even and odd fibre Flat Field frames by the full slit Flat Field frame	• (ready) even fibres Flat Field frame [out3.2] • (ready) odd fibres Flat Field Frame [out3.2]	MIDAS
Standard extraction				

Stage	Input	Operation	Output	Proc.
3.3	• even-fibres Flat Field frame [out3.2] • odd-fibres Flat Field frame [out3.2] • Order-fibre polynomial solution [out2.2]	Construction of preliminary single-fibre Flat Field frames, by simple selection of the appropriate portions of background-subtracted even and odd-fibre Flat Field frame and zeroing of the rest	• n (preliminary, background-subtracted) single-fibre Flat Field frames [out3.3]	NEW
3.4	• n (preliminary, background-subtracted) single-fibre Flat Field frames [out3.3] • bad pixels Mask [database] • Order-fibre polynomial solution [out2.2]	Construction of single fibre Flat Field frames cleaned from hot/dead pixels	• n (cleaned) single-fibre Flat Field frames [out3.4]	NEW
3.5	• all-fibres Flat Field frame [out1.2] • bad pixels Mask [database] • Inter-order table [out2.2]	Preliminary computation and subtraction of the scattered light	• (background subtracted) all-fibres Flat Field frame [out3.5]	MIDAS
3.6	• (background subtracted) all fibres Flat Field frame [out3.5] • (inter.) full slit Flat Field frame [out1.2]	Division of all fibre Flat Field frames by the full slit Flat Field frame	• (preliminary flat-fielded) all fibres Flat Field frame [out3.6]	MIDAS
Standard extraction				

Stage	Input	Operation	Output	Proc.
3.7	• (preliminary flat-fielded) all-fibres Flat Field frame [out3.6] • n (cleaned) single-fibre Flat Field frames [out3.4] • Order-fibre polynomial solution [out2.2]	All fibres Flat Field frame shift determination by computing its cross-correlation with the single fibre Flat Field frames	• n (convolved) single-fibre Flat Field frames [out3.7] • cross correlation table [out3.7]	NEW
3.8	• all-fibres Flat Field frame [out1.2] • bad pixels Mask [database] • Inter-order Table [out2.2] • cross correlation table [out3.7]	Final computation of the scattered light in the all-fibres Flat Field Frame, using inter-order positions corrected for the drift, and its subtraction (*to do only if the drift is significant, else keep the previous preliminary background subtraction*)	• all-fibres Flat Field frame [out3.8]	NEW
3.9	• (background subtracted) all fibres Flat Field frame [out3.8] • (inter.) full slit Flat Field frame [out1.2]	Division of all fibre Flat Field frames by the full slit Flat Field frame (*to do only if the background was recomputed in the preceding step, else keep the preliminary one*)	• (ready) all fibres Flat Field frame [out3.9]	MIDAS
Standard extraction				

Stage	Input	Operation	Output	Proc.
3.10	• all-fibres Flat Field frame [out3.9] • n single-fibre Flat Field frames [out3.4] • bad pixels Mask [database] • Order-fibre Table [out2.2] • Order-fibre polynomial solution [out2.2]	Integration over fixed y-intervals and determination of the preliminary Illumination Fractions	• n^2 frames containing (preliminary) Illumination Fractions [out3.10] • n frames containing (blended) throughput corrections [out3.10]	mod. MIDAS
3.11	• n 1D frames containing throughput corrections [out3.10] • n^2 1D frames containing Illumination Fractions [out3.10]	Deblending of the throughput corrections	• n 1D frames containing (deblended) throughput corrections [out3.11]	mod. NEW
3.12	• n 1D frames containing throughput corrections [out3.11] • n single-fibre Flat Field frames [out3.4] • bad pixels Mask [database] • Order-fibre polynomial solution [out2.2]	Construction of corrected, background subtracted single fibre Flat Field frames	• n (corrected) single fibre Flat Field frames (pixel-order space) [out3.12]	mod. NEW
Standard extraction				

Stage	Input	Operation	Output	Proc.
4.1	• Science frame [out1.2] • bad pixels Mask [database]	Cosmic ray hits detection and flagging	• (updated) bad pixels mask [out4.1]	mod. MIDAS
4.2	• Science frame [out4.1] • Th-Ar frame [out1.2] • bad pixels Mask [database] • Inter-order table [out2.2]	Preliminary computation and subtraction of the scattered light	• (background subtracted) Science frame [out4.2] • (background subtracted) Th-Ar frame [out4.2]	MIDAS
4.3	• (background subtracted) Science frame [out4.2] • (background subtracted) Th-Ar frame [out4.2] • (inter.) full slit Flat Field frame [out1.2]	Division of Science and Th-Ar frames by the full slit Flat Field frame	• (preliminary flat-fielded) Science frame [out4.3] • (preliminary flat-fielded) Th-Ar frame [out4.3]	MIDAS
Standard extraction				

Stage	Input	Operation	Output	Proc.
4.4	• (preliminary flat-fielded) Science frame [out4.3] • (preliminary flat-fielded) Th-Ar frame [out4.3] • n (cleaned) single-fibre Flat Field frames [out3.12] • Order-fibre polynomial solution [out2.2]	Science and Th-Ar frame shift determination by computing their cross-correlation with the single fibre Flat Field frames	• n (convolved) single-fibre Flat Field frames [out4.4] • cross correlation table [out4.4]	NEW
4.5	• Science frame [out1.2] • Th-Ar frame [out1.2] • bad pixels Mask [database] • Inter-order Table [out2.2] • cross correlation table [out4.4]	Final computation of the scattered light in the Science and Th-Ar Frame, using inter-order positions corrected for the drift, and its subtraction (*to do only if the drift is significant, else keep the previous preliminary background subtraction*)	• Science frame [out4.5] • Th-Ar frame [out4.5]	NEW
Standard extraction				

Stage	Input	Operation	Output	Proc.
4.6	• (background sub-tracted) Science frame [out4.5] • (background sub-tracted) Th-Ar frame [out4.5] • (inter.) full slit Flat Field frame [out1.2]	Division of Science and Th-Ar frames by the full slit Flat Field frame (*to do only if the background was recomputed in the preceding step, else keep the preliminary one*)	• (ready) Science frame [out4.6] • (ready) Th-Ar frame [out4.6]	MIDAS
4.7	• Science frame [out4.6] • Th-Ar frame [out4.6] • n single fibre Flat Field frames [out4.4] • bad pixels Mask [out4.1] • Order-fibre polynomial solution [out2.2]	Integration over fixed y-intervals and determination of the Illumination Fractions	• n^2 frames containing Illumination Fractions [out4.7] • n (blended) Science spectra (pixel-order space) [out4.7] • n (blended) Th-Ar spectra (pixel-order space) [out4.7] • Used flux fraction [out4.7]	mod. MIDAS
4.8	• n Science spectra [out4.7] • n Th-Ar spectra [out4.7] • n^2 frames containing Illumination Fractions [out4.7] • bad pixels Mask [out4.1]	Deblending of the fibres in Th-Ar and Science frames	• n (deblended) Science spectra (pixel-order space) [out4.8] • n (deblended) Th-Ar spectra (pixel-order space) [out4.8]	mod. NEW

Standard extraction

Stage	Input	Operation	Output	Proc.
5.1	• n Th-Ar spectra [out4.8] • simultaneous calibration spectrum [out4.8] • 1st guess wavelength calibration solution [out2.1]	Computation of the uncorrected wavelength calibration solutions	• Wavelength calibration solutions [out5.1]	mod. MIDAS
5.2	• n Wavelength calibration solutions from the Th-Ar frame [out4.1] • Wavelength calibration solution from the simultaneous calibration fibre[out4.1]	Computation of the higher order correction to the n wavelength calibration solutions from the difference in the ones for the simultaneous calibration fibre (*only in simultaneous calibration mode*)	• n (corrected) Wavelength calibration solutions [out5.2]	NEW
5.3	• n Science spectra (pixel-order space) [out4.8] • n wavelength calibration solutions [out5.1] or [out5.2]	Rebinning of Science spectra	• n (Rebinned) Science spectra (wavelength-order space) [out5.3]	MIDAS
6.1	• $n-1$ Science spectra (wavelength-order space) [out5.3] • Sky Spectrum (wavelength-order space) [out5.3]	Sky subtraction (if requested)	• $n-1$ (sky subtracted) Science Spectra (wavelength-order space) [out5.3]	MIDAS
Standard extraction				

Stage	Input	Operation	Output	Proc.
7.1	• Science spectra [5.3 or 6.1]	Order merging	• Final Science spectra [out7.1]	MIDAS
Standard extraction				

6.3 Optimal extraction

Stage	Inputs	Operation	Output	Proc.
1.1	• raw Bias frame(s) [calibrations] • raw Dark Current Frame [calibrations] • raw even-fibres Flat Field frame(s) [calibrations] • raw odd-fibres Flat Field frame(s) [calibrations] • raw all-fibres Flat Field frame(s) [calibrations] • raw full slit Flat Field frame(s) [calibrations]	Construction of master Bias, Dark Current and Flat Field frames, cleaned from cosmic ray hits	• (master) Bias frame [out1.1] • (master) Dark Current frame [out1.1] • (cleaned) even-fibres Flat Field frame [out1.1] • (cleaned) odd-fibres Flat Field Frame [out1.1] • (cleaned) all-fibres Flat Field frame [out1.1] • (cleaned) full slit Flat Field frame [out1.1]	MIDAS

Optimal extraction

Stage	Inputs	Operation	Output	Proc.
1.2	• Bias frame [out1.1] • Dark Current frame [out1.1] • raw Science frame [observations] • raw Th-Ar frame [calibrations] • even-fibres Flat Field frame [out1.1] • odd-fibres Flat Field Frame [out1.1] • all-fibres Flat Field frame [out1.1] • full slit Flat Field frame [out1.1]	Subtraction of the bias and dark current values from the Science and calibration frames	• (inter.) Science frame [out1.2] • (inter.) Th-Ar frame [out1.2] • (inter.) even fibres Flat Field frame [out1.2] • (inter.) odd fibres Flat Field Frame [out1.2] • (inter.) all fibres Flat Field frame [out1.2] • (inter.) full slit Flat Field frame [out1.2]	MIDAS
2.1	• single fibre Th-Ar frame [database] • bad pixels Mask [database]	Format check	• 1st guess wavelength calibration solution [out2.1] • 1st guess order finding [out2.1]	**UVES** context
Optimal extraction				

Stage	Inputs	Operation	Output	Proc.
2.2	• even-fibres Flat Field frame [out1.2] • odd-fibres Flat Field frame [out1.2] • bad pixels Mask [database] • 1st guess order finding [out2.1]	Definition of the positions of orders and fibres on the frame	• Order-fibre Table [out2.2] • Inter-order Table [out2.2] • Order-fibre polynomial solution [out2.2]	mod. MIDAS
3.1	• even-fibres Flat Field frame [out1.2] • odd-fibres Flat Field frame [out1.2] • bad pixels Mask [database] • Inter-order table [out2.2]	Computation and subtraction of the scattered light in the even and odd-fibres Flat Field frames, by fitting a low degree polynomial to inter-order positions	• (background subtracted) even-fibres Flat Field frame [out3.1] • (background subtracted) odd-fibres Flat Field frame [out3.1]	MIDAS
3.2	• (inter.) even fibres Flat Field frame [out3.1] • (inter.) odd fibres Flat Field Frame [out3.1] • (inter.) full slit Flat Field frame [out1.2]	Division of even and odd fibre Flat Field frames by the full slit Flat Field frame	• (ready) even fibres Flat Field frame [out3.2] • (ready) odd fibres Flat Field Frame [out3.2]	MIDAS
Optimal extraction				

Stage	Inputs	Operation	Output	Proc.
3.3	• even-fibres Flat Field frame [out3.2] • odd-fibres Flat Field frame [out3.2] • Order-fibre polynomial solution [out2.2]	Construction of preliminary single-fibre Flat Field frames, by simple selection of the appropriate portions of background-subtracted even and odd-fibre Flat Field frame and zeroing of the rest	• n (preliminary, background-subtracted) single-fibre Flat Field frames [out3.3]	NEW
3.4	• n (preliminary, background-subtracted) single-fibre Flat Field frames [out3.3] • bad pixels Mask [database] • Order-fibre polynomial solution [out2.2]	Construction of single fibre Flat Field frames cleaned from hot/dead pixels	• n (cleaned) single-fibre Flat Field frames [out3.4]	NEW
3.5	• all-fibres Flat Field frame [out1.2] • bad pixels Mask [database] • Inter-order table [out2.2]	Preliminary computation and subtraction of the scattered light	• (background subtracted) all-fibres Flat Field frame [out3.5]	MIDAS
3.6	• (background subtracted) all fibres Flat Field frame [out3.5] • (inter.) full slit Flat Field frame [out1.2]	Division of all fibre Flat Field frames by the full slit Flat Field frame	• (preliminary flat-fielded) all fibres Flat Field frame [out3.6]	MIDAS
Optimal extraction				

Stage	Inputs	Operation	Output	Proc.
3.7	• (preliminary flat-fielded) all-fibres Flat Field frame [out3.6] • n (cleaned) single-fibre Flat Field frames [out3.4] • Order-fibre polynomial solution [out2.2]	All fibres Flat Field frame shift determination by computing its cross-correlation with the single fibre Flat Field frames	• n (convolved) single-fibre Flat Field frames [out3.7] • cross correlation table [out3.7]	NEW
3.8	• all-fibres Flat Field frame [out1.2] • full slit Flat Field frame [out1.2] • n single-fibre Flat Field frames [out3.4] • bad pixels Mask [database] • Inter-order Table [out2.2] • cross correlation table [out3.7]	Final computation of the scattered light in the ready all-fibres Flat Field Frame, by fitting a low degree polynomial to inter-order positions and possibly a few positions below the bluest orders, with simultaneous optimal extraction of the spectra only in those positions and its subtraction	• (ready) all-fibres Flat Field frame [out3.8]	NEW
3.9	• (background subtracted) all fibres Flat Field frame [out3.8] • (inter.) full slit Flat Field frame [out1.2]	Division of all fibre Flat Field frames by the full slit Flat Field frame	• (ready) all fibres Flat Field frame [out3.9]	MIDAS
Optimal extraction				

Stage	**Inputs**	**Operation**	**Output**	**Proc.**
3.10	• all-fibres Flat Field frame [out3.9] • n single-fibre Flat Field frames [out3.4] • bad pixels Mask [database] • Order-fibre Table [out2.2] • Order-fibre polynomial solution [out2.2]	Evaluation of the relative throughputs of the fibres applying the "Optimal Extraction" to the all-fibres Flat Field Frame	• n frames containing throughput corrections [out3.10]	NEW
3.11	• n frames containing throughput corrections [out3.10] • n single-fibre Flat Field frames [out3.3] • bad pixels Mask [database] • Order-fibre polynomial solution [out2.2]	Construction of throughput corrected, background subtracted single-fibre Flat Field frames	• n (corrected) single-fibre Flat Field Frames (pixel-order space) [out3.11]	NEW

Optimal extraction

Stage	Inputs	Operation	Output	Proc.
4.1	• Science frame [out1.2] • Th-Ar frame [out1.2] • bad pixels Mask [database] • Inter-order table [out2.2]	Preliminary computation and subtraction of the scattered light	• (background subtracted) Science frame [out4.1] • (background subtracted) Th-Ar frame [out4.1]	MIDAS
4.2	• (background subtracted) Science frame [out4.1] • (background subtracted) Th-Ar frame [out4.1] • (inter.) full slit Flat Field frame [out1.2]	Division of Science and Th-Ar frames by the full slit Flat Field frame	• (preliminary flat-fielded) Science frame [out4.2] • (preliminary flat-fielded) Th-Ar frame [out4.2]	MIDAS
4.3	• (preliminary flat-fielded) Science frame [out4.2] • (preliminary flat-fielded) Th-Ar frame [out4.2] • n (cleaned) single-fibre Flat Field frames [out3.11] • Order-fibre polynomial solution [out2.2]	Science and Th-Ar frame shift determination by computing their cross-correlation with the single fibre Flat Field frames	• n (convolved) single-fibre Flat Field frames [out4.3] • cross correlation table [out4.3]	NEW
Optimal extraction				

Stage	Inputs	Operation	Output	Proc.
4.4	• Science frame [out1.2] • Th-Ar frame [out1.2] • full slit Flat Field frame [out1.2] • n single-fibre Flat Field Frames [out4.3] • bad pixels Mask [database] • Inter-order Table [out2.2] • cross correlation table [out4.3] • Order-fibre polynomial solution [out2.2]	Final computation of the scattered light in the Science frame and Th-Ar frame, by fitting a low degree polynomial to inter-order positions and possibly a few positions below the bluest orders, with simultaneous optimal extraction of the spectra only in those positions	• (background subtracted) Science frame [out4.4] • (background subtracted) Th-Ar Frame [out4.4]	NEW
4.5	• (background subtracted) Science frame [out4.4] • (background subtracted) Th-Ar frame [out4.4] • (inter.) full slit Flat Field frame [out1.2]	Division of Science and Th-Ar frames by the full slit Flat Field frame	• (ready) Science frame [out4.5] • (ready) Th-Ar frame [out4.5]	MIDAS
Optimal extraction				

Stage	Inputs	Operation	Output	Proc.
4.6	• Science Frame [out4.5] • Th-Ar Frame [out4.5] • n single-fibre Flat Field frames [out3.3] • bad pixels Mask [database] • Order-fibre polynomial solution [out2.2]	Optimal Extraction	• n Science Spectra (pixel-order space) [out4.6] • n Th-Ar spectra (pixel-order space) [out4.6] • Quality controls #1 and #2 [out4.6]	NEW
5.1	• n Th-Ar spectra [out4.8] • simultaneous calibration spectrum [out4.8] • 1st guess wavelength calibration solution [out2.1]	Computation of the uncorrected wavelength calibration solutions	• Wavelength calibration solutions [out5.1]	mod. MIDAS
5.2	• n Wavelength calibration solutions from the Th-Ar frame [out4.1] • Wavelength calibration solution from the simultaneous calibration fibre[out4.1]	Computation of the higher order correction to the n wavelength calibration solutions from the difference in the ones for the simultaneous calibration fibre (*only in simultaneous calibration mode*)	• n (corrected) Wavelength calibration solutions [out5.2]	mod. MIDAS

Optimal extraction

Stage	Inputs	Operation	Output	Proc.
5.3	• n Science spectra (pixel-order space) [out4.8] • n wavelength calibration solutions [out5.1] or [out5.2]	Rebinning of Science spectra	• n (Rebinned) Science spectra (wavelength-order space) [out5.3]	NEW
6.1	• $n-1$ Science spectra (wavelength-order space) [out5.3] • Sky Spectrum (wavelength-order space) [out5.3]	Sky subtraction (if requested)	• $n-1$ (sky subtracted) Science Spectra (wavelength-order space) [out5.1]	MIDAS
7.1	• Science spectra [[out5.3] or [out6.1]]	Order merging	• Final Science spectra [out7.1]	MIDAS
Optimal extraction				

7 Breakdown of reduction steps

In the following you can find a detailed breakdown of each reduction step with the needed inputs and the generated outputs, its purpose and a verbose description of its usage.

In spite of the fact that it is not shown explicitly, to reduce the clutter, each procedure keeps trace of the errors present in the initial frames by calculating the error propagated to each output. Therefore, to each output frame, be it in pixel-pixel, pixel-order, wavelength-order or wavelength space, will be associated another frame of the same size and in the same space, containing the estimated error.

A block diagram of the procedure is also included with the following graphic conventions:

- A circle stands the procedure itself
- A rounded box stands for inputs which are the MIDAS frames (`.bdf`)
- An ellipse stands for inputs which are from the **UVES** database (even when it was modified by another procedure)
- An hexagon stands for inputs which are MIDAS tables (`.tbl`) or descriptors

7.1 Preliminary cleaning by stacking

Purpose:

Produce frames free from cosmic ray hits before further processing

Used in:

- step 1.1
- possibly step 4.1 (standard reduction) if multiple exposures of the same Science frame are available

Inputs:

1. 3 or more subsequent exposures of the same frame
2. CCD parameters such as R.O.N. and gain (probably stored in image descriptors)

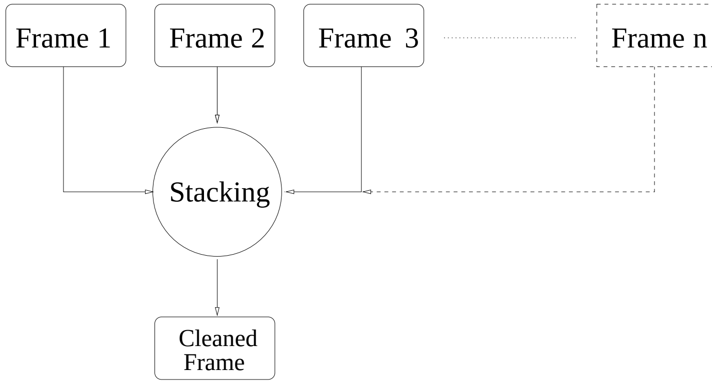

Figure 7.1: Rejection of cosmic rays by stacking of frames

Outputs:

1. 1 averaged frame with cosmic ray hits removed

Description:

Common image stacking techniques with sigma clipping (already implemented in existing MIDAS commands) are used to obtain an average image without cosmic ray hits. At least 3 instances of the same frame are needed, 5 are recommended.

7.2 Bias and Dark Current subtraction

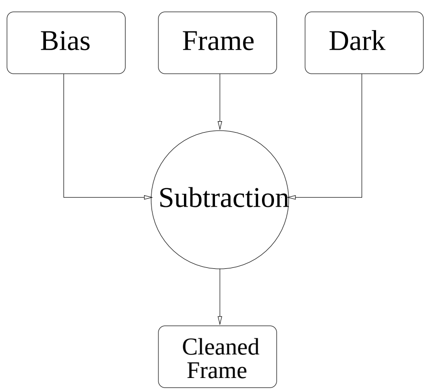

Figure 7.2: Bias and Dark Current subtraction

Purpose:

Subtract Bias and Dark current from other calibration frames and Science frames

Used in:

- step 1.2

Inputs:

1. master Bias frame
2. master Dark Current frame, with its exposure time stored in its descriptors
3. a Science frame (or any other frame from which Bias and Dark Current have to be subtracted), with its exposure time stored in its descriptors

Outputs:

1. 1 Bias and Dark Current subtracted Science (or other) frame

Description:

Using standard MIDAS commands, the Bias frame is subtracted from both the Science frame and the Dark Current frame. The resulting Dark Current frame is then scaled depending on the ratio between its exposure time and that of the Science frame, from which is then subtracted.

7.3 Format check

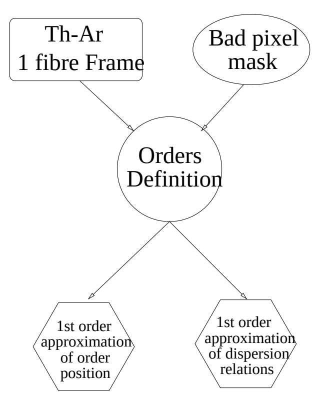

Figure 7.3: First order approximations of the positions of the orders

Purpose:

Construction of 1st order approximations for the positions of the orders on the frame and dispersion relations

Used in:

- step 2.1

Inputs:

1. single fibre Th-Ar frame
2. bad pixels mask

Outputs:

1. 1st order approximation for the positions of the orders in the frame
2. 1st order approximation for the dispersion relations

Description:

This step, part of the already existing **UVES** context, compares a single fibre Th/Ar frame (a narrow slit Th/Ar frame in the existing pipeline) with a physical model of UVES, and derives 1st order approximations for the positions of the orders on the frame and dispersion relations. It is expected to work out of the box, as a single fibre frame differs very little from a narrow slit frame.

7.4 Orders definition

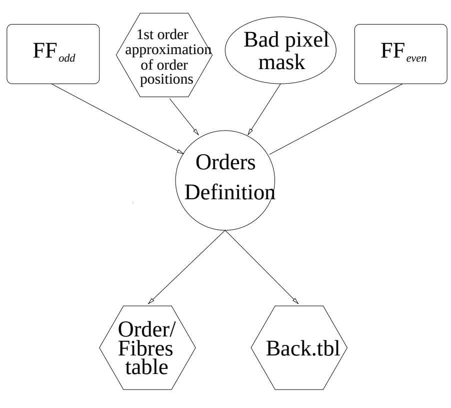

Figure 7.4: Finding fibres and orders positions

Purpose:

Definition of the positions of orders and fibres on the frame

Used in:

- step 2.2

Inputs:

1. even fibres Flat Field frame
2. odd fibres Flat Field frame
3. 1st order approximation for the positions of the orders in the frame
4. bad pixels mask

Outputs:

1. Order/fibres table, including (as descriptors) the parameters for the polynomial solution
2. "Back.tbl" table, containing a list of inter-order intervals on the frames which can be used for subsequent background estimation

Description:

This part is very similar to the one already implemented in the DEFINE/HOUGH command of the echelle context of MIDAS. Its first few steps will be exactly equal to those in DEFINE/HOUGH, apart from the fact that they will be run on two frames (the even fibres Flat Field frame and the odd fibres Flat Field frame) instead of one only:

- Make a rough estimation of the background, by median filtering over running boxes and choosing the lowest value found, and subtract it (just as in DEFINE/HOUGH, but do it separately for the two input frames).
- Perform a Hough transform and, on the result, find the clusters corresponding to approximately straight lines, thereby obtaining a table of angular coefficients and intercepts, sorted by intercepts, one for each straight line found. Trace these approximate "lines", each corresponding to an order of a fibre, on the corresponding Flat Field frame, and build a table containing, for each "line", a list of x-y couples following the maxima on the frame. Again, this step is exactly equal to what is done in DEFINE/HOUGH, perhaps with some very minor tweaking of the internal parameters, but it is applied independently to the odd fibre and even fibre Flat Field frames. The result of this step is a table of x-y couples (one per table line), each one tagged with a unique number identifying the "line" to which it belongs.
- Merge the last two tables resulting from the step above, sorting them in the order of the intercepts of the "lines" to which the x-y couples belong. This can be easily accomplished by a couple of simple MIDAS commands.

- Use the 1st approximation of the order position from the format check to assign an order number and a fibre number to each "line" traced in the above table. While this is conceptually easy to do, it does not exist yet in MIDAS, and it will be implemented as a C module. As a result, the table will get two additional columns, one containing the order number and one containing the fibre number of a given x-y couple (a line of the table).
- Making use of the facts that the n different fibres in the same order must be parallel and that their distances must be fixed constants, fit the traces in the table with one bivariate polynomial in the pixel-order space and $n-1$ offsets. This is a linear fit, which can be solved analytically by a simple matrix inversion, and will require the use of a standard library of numerical routines (e. g. Numerical Recipes).
- Making use of the result of the above step, build a table containing a list of fitted orders/fibres positions (just as is done at the end of the DEFINE/HOUGH procedure with orders) to be used for subsequent processing, and store the results of the fit as descriptors of this table. Likewise, build a table defining a list of rectangular intervals of x-y coordinates that only contain inter-order points. This latter table will be structured *exactly* as the "back.tbl" produced by the DEFINE/HOUGH command, in order to be compatible out of the box with existing MIDAS commands for background estimation.

7.5 Division by the full slit Flat Field

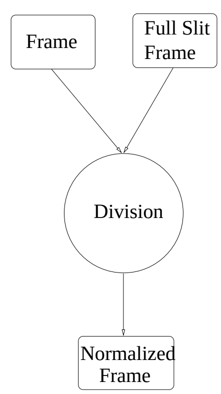

Figure 7.5: Division by the full slit FF

Purpose: Divide all the calibration and science frames by the full slit Flat Field frame

Used in:

- step 1.6

Inputs:

1. Science Frame
2. Th-Ar Frame
3. even fibres Flat Field
4. odd fibres Flat Field
5. all fibres Flat Field
6. full slit Flat Field

Outputs:

1. Science Frame
2. Th-Ar Frame
3. even fibres Flat Field
4. odd fibres Flat Field
5. all fibres Flat Field

Description: Using standard MIDAS commands, the calibration and Science frames are divided by the full slit frame in order to remove any pixel to pixel variation.

7.6 Single fibre Flat Field Frames Cleaning

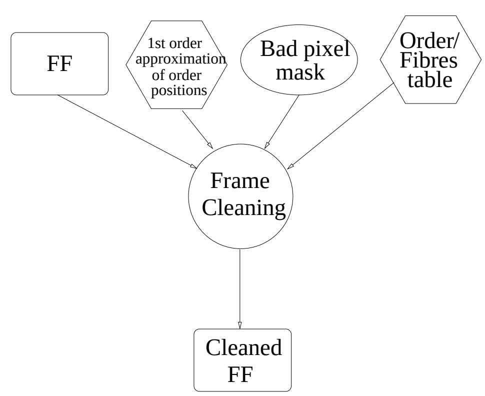

Figure 7.6: Construction of single fibre Flat Field cleaned by hot/dead pixels

Purpose:

Construction of single fibre Flat Field cleaned by any hot/dead pixels

Used in:

- step 3.4

Inputs:

1. n single-fibre Flat Field frames
2. bad pixels Mask
3. Order-fibre polynomial solution
4. Inter-order table

Outputs:

1. n normalised single-fibre Flat Field frames
2. n 1D single fibre normalisation factors
3. even fibres Flat Field frame
4. odd fibres Flat Field frame
5. all fibres Flat Field frame

Description:

This step has the purpose to obtain single fibre Flat Fields with as little as possible (ideally none) hot/dead pixel in any position of the frame, in order to have for every x, order and fibre in the frame a clean cross-dispersion PSF. This task is accomplished under the assumption that the fibre cross-dispersion PSF is insensitive to variation of ~20 pixels in the dispersion (x) direction.

For every given order m, we factor the F'_n frames in the following way:

$$\mathrm{F}'(x, y) = \mathrm{N}(x)\mathrm{PSF}(x, y), \tag{7.1}$$

where, for the sake of simplicity, the n and m indexes are implicit and have been dropped. The x-dependent normalisation factor $\mathrm{N}(x)$ is straightforwardly evaluated as

$$\mathrm{N}(x) = \sum_y \mathrm{F}'(x, y), \tag{7.2}$$

when there are no bad pixels for the given n, m and x. To fill in the "holes" we proceed in the following way: since the y position of the orders, as a function of x, can be locally described with great accuracy by a straight line with a slope s (dependent on m and, even if very weakly, on x) always < 0.039, it is always possible to find a $\delta x = \frac{1}{s}$ so that

$$\mathrm{PSF}(x, y) \simeq \mathrm{PSF}(x \pm \delta x, y \pm 1). \tag{7.3}$$

The δx can be truncated to the nearest integer value introducing a negligible error in the above equation. Therefore, when $\mathrm{F}'_n(x, y)$ is incomplete for a given x, we look at $\mathrm{F}'_n(x \pm \delta x, y \pm 1)$ and find the subset **S** of y pixels present in $\mathrm{F}'_n(x, y)$ and for which the corresponding shifted pixel in $\mathrm{F}'_n(x \pm \delta x, y \pm 1)$ is also present. Then temporary normalisation factors $\mathrm{N}'(x)$ and $\mathrm{N}'(x \pm \delta x)$ are calculated using the equation

$$\mathrm{N}'(x) = \sum_{y \in \mathbf{S}} \mathrm{F}'(x, y) \tag{7.4}$$

which is obtained from equation 7.2 by restricting the sum only to pixels belonging to the subset **S**. This in turn leads to the following equation

$$\mathrm{F}'(x, y) \simeq \frac{\mathrm{N}'(x)}{\mathrm{N}'(x \pm \delta x)} \mathrm{F}'(x \pm \delta x, y \pm 1), \tag{7.5}$$

which provides estimates for the missing pixels.

Where two such estimates are possible (everywhere except the edges of an order in x and the unfortunate case of two bad pixels that are one at the shifted position of the other), a weighted average is performed, otherwise the single available estimate is taken, or the pixel is skipped if there is no available estimate (which is *very* unlikely). In this way, in a single pass, some missing (bad) pixels are filled in. This “filling in” procedure is iterated until no more holes can be filled, either because there are none left or because there are no available estimates for them.

While *extremely* unlikely, as it would require many bad pixels to be placed in a very well defined order by chance, it may in principle happen that some holes still remain at the end of this procedure. In this case, a warning will be issued, and, as a fall-back solution, the missing pixels and normalisation factors will be interpolated from neighbouring ones. This will be less accurate, but will permit to still extract meaningful spectra at the affected x and m. Should this interpolation still fail, a more serious warning will be issued and the whole x slice of pixels in the m order will be marked as bad.

For all complete x slices, the normalisation factors $\mathrm{N}(x)$ are calculated using equation 7.2.

7.7 Cleaning of Science frames by filtering

Purpose:

Clean Science frames from cosmic ray hits before further processing

Used in:

- step 4.1 (standard extraction)

Inputs:

1. Science frame
2. CCD parameters such as R.O.N. and gain (probably stored in image descriptors)
3. bad pixels Mask

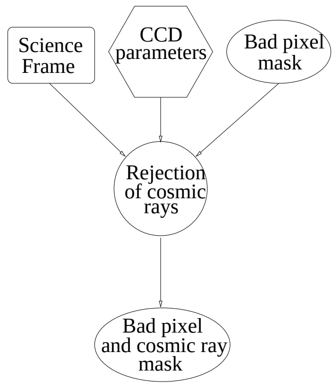

Figure 7.7: Filtering Science Frames for cosmic ray hits

Outputs:

1. updated bad pixels mask with cosmic ray hits included (specific for this Science frame only)

Description:

In standard reduction, cosmic ray hits cannot be identified during the extraction step, therefore they must be eliminated beforehand. If multiple exposures of the same Science frame are available, this is accomplished by stacking as described in section (insert section here), otherwise a filter (e. g. a running median over an appropriate window) must be used to identify cosmic ray hits. This is possible, to some extent, thanks to the relatively large sampling of UVES in fibre mode. These pixels cannot be given a sensible value if only one exposure is available. Therefore, a mask of pixels to reject is built and merged with the bad pixels mask, and will be used throughout the remaining steps *for this Science frame only.*

7.8 Standard background estimation and subtraction

Purpose:

Estimation, with standard techniques, of the scattered light over Science, Flat Field or Th/Ar frames, and its subsequent subtraction

Used in:

- step 3.1
- step 4.1 (standard extraction)

Inputs:

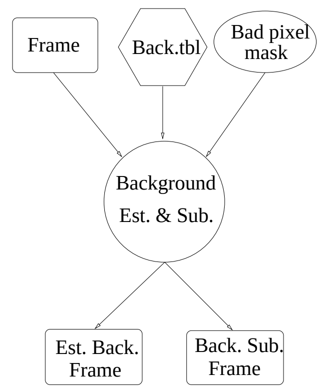

Figure 7.8: Standard background estimation and subtraction

1. Science or Flat Field or Th/Ar frame
2. bad pixels mask
3. "Back.tbl" table

Outputs:

1. estimated Background frame
2. background subtracted frame

Description:

Existing facilities of the echelle context of MIDAS, such as the BACKGROUND/ECHELLE command, are used to estimate the scattered light. Standard MIDAS commands (e. g. COMPUTE/IMAGE) can then be used to subtract it from the original frame. This sequence of operations is already implemented in the higher level command SUBTRACT/BACKGROUND of the echelle context of MIDAS. Minor modifications to these procedures may be performed in order to make use of the bad pixels mask (i. e. to avoid using pixels known to be bad in background estimation).

7.9 Science Frame shift determination

Purpose:

Estimation of the shift that affects the Science Frame respect to the Flat Fields

Used in:

- step 3.4 (standard extraction)
- step 3.3 (optimal extraction)

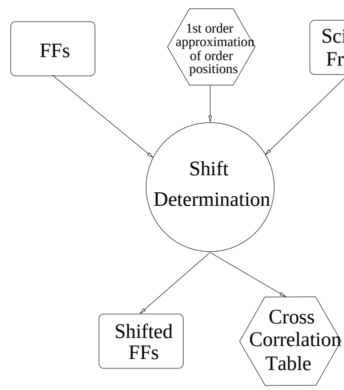

Figure 7.9: Shift Determination

Inputs:

1. even-fibres Flat Field frame
2. odd-fibres Flat Field frame
3. all-fibres Flat Field frame
4. n single-fibre Flat Field frames
5. Science frame
6. Order-fibre polynomial solution

Outputs:

1. all-fibres Flat Field frame
2. n single-fibre Flat Field frames
3. cross correlation table

Description:

Thanks to the slight slope of the echelle orders, a small shift in y of the Science frame with respect to the FF frames is nearly equivalent to a shift along x between these frames, at the expense of very few pixels at the frame borders. To compute the needed amount of shift to be applied, a correlation function is computed between the Science frame and the FF frames, order by order, for a varying amount of x shift. The shift values (one per order) yielding a maximum in the correlation function are then used to reconstruct new FF frames, appropriate for the Science frame at hand. These values are also logged in a table. This will be implemented as a new C module of MIDAS.

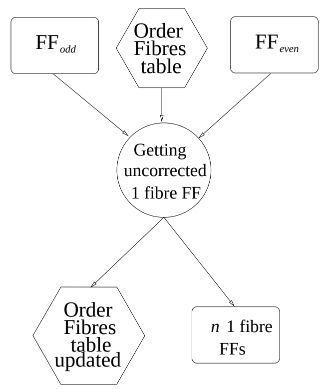

Figure 7.10: Extracting raw single fibre Flat Field

7.10 Preliminary cut of single fibre flat field frames

Purpose:

Construction of background subtracted single fibre Flat Field frames, uncorrected for the relative throughputs of adjacent fibres

Used in:

- step 3.3

Inputs:

1. background subtracted even fibres Flat Field frame
2. background subtracted odd fibres Flat Field frame
3. Orders/fibres table

Outputs:

1. n preliminary, background subtracted single fibre Flat Field frames
2. updated orders/fibres table

Description:

For each fibre i, an interval δ in y around the position of its orders on the frame (as contained in the orders/fibres table) is defined so that it contains all of the light from that fibre. Then the even or odd fibres Flat Field frame containing that fibre is copied to a new frame, and all pixels outside the interval defined above are set to 0 (zero). In this way a frame containing the contribution of a single fibre to the Flat Field is obtained. The values defining the start and end of the intervals are stored as descriptors or in new columns in the orders/fibres table (TBD).

7.11 Integration over fixed y intervals

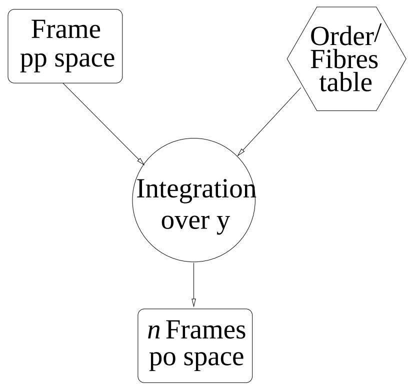

Figure 7.11: Integration of the single fibre signal

Purpose:

Simple integration of the signal in the interval covered by every single fibre, order by order

Used in:

- step 3.10 (standard extraction)
- step 4.7 (standard extraction)

Inputs:

1. a frame in pixel-pixel space
2. Orders/fibres table

Outputs:

1. n frames in pixel-order space

Description:

For each fibre i of the n present, for every order m an integration over a "numerical slit" covering the fibre i is performed over the input frame. This can be accomplished by a simple procedure that loops over fibres and feeds appropriate input to the EXTRACT/ORDER procedure of the echelle context of MIDAS. This involves extracting from the orders/fibres table a subtable containing all the orders of fibre i only, which is easily accomplished by straightforward MIDAS table manipulation commands.

This step produces conceptually different results depending on the frame to which it is applied:

- if applied to a Science or Th/Ar or all fibres Flat Field frame, the description given above holds;
- if applied to the single fibre Flat Field frame of fibre i it will give n pixel-order frames containing the illumination fractions of fibre i over the intervals of all fibres.

7.12 Deblending of standard extracted spectra

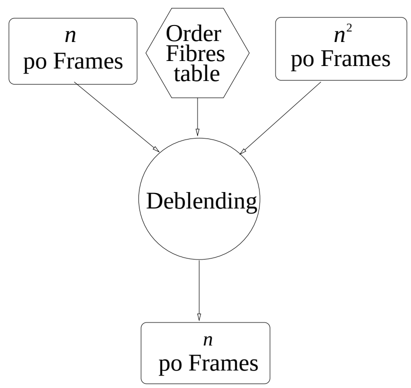

Figure 7.12: Deblending of standard extracted spectra

Purpose:

Disentangle the contributions from different fibres

Used in:

- step 3.11 (standard extraction)
- step 4.7 (standard extraction)

Inputs:

1. n frames in pixel-pixel space resulting from integration over fixed intervals of a Science, Th/Ar or all fibres Flat Field frame
2. n^2 frames in pixel-order space resulting from integration over fixed intervals of n single fibre Flat Field frames
3. Orders/fibres table

Outputs:

1. n frames in pixel-order space containing disentangled contributions

Description:

As described in section 5.7.2 (see equations therein), for each given order m and wavelength pixel j, the result c_n^o of the integration of flux in a frame to be reduced over the window of width w centred on fibre n will be composed of a linear combination of the fluxes coming from the fibre n itself and neighbouring ones, with coefficients $A(n, n')$. These latter coefficients represent the contribution of fibre n' to the integral centred over fibre n, and can be obtained straightforwardly integrating the single fibre flat field frame $\mathrm{FF}_{n'}$ over the interval centred on fibre n, using the very same procedure used for integration on the frame to be reduced and *discarding the same set of bad pixels.* The recovery of the true fluxes $c_{n'}$ entering the linear combination involves the solution of the system of linear equations in equation 5.14, involving the inversion of the $A(n, n')$ matrices. A module, making use of library functions for the matrix inversions, will be written for this purpose.

7.13 Construction of single fibre flat field frames

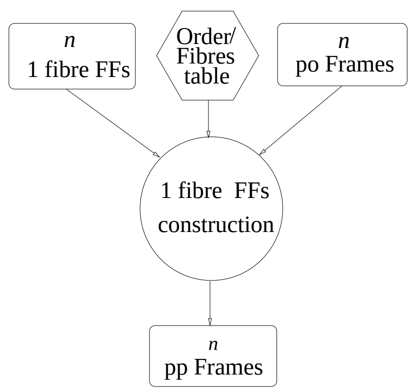

Figure 7.13: Construction of background subtracted single fibre FFs

Purpose:

Construction of background subtracted single fibre Flat Field frames, corrected for the relative throughputs of adjacent fibres

Used in:

- step 3.12 (standard extraction)
- step 3.11 (optimal extraction)

Inputs:

1. n preliminary background subtracted single fibre Flat Field frame

2. n pixel-order frames containing the n "spectra" fully extracted from the all fibres Flat Field frame using the preliminary single fibre Flat Field frames to evaluate the illumination fractions
3. Orders/fibres table

Outputs:

1. n background subtracted single fibre Flat Field frames, corrected for the relative throughputs of the fibres

Description:

The n "spectra" fully extracted from the all fibres Flat Field frame using the corrected single fibre Flat Field frames to evaluate the illumination fractions would be identically equal to 1 by definition. This means that the corrected single fibre Flat Field frames can be obtained simply multiplying all the pixels of every order of the preliminary single fibre Flat Field frames by the value at the same pixel and order of the corresponding "spectrum" extracted from the all fibres Flat Field frame. This will need to be implemented in a new C module or in a MIDAS procedure (TBD).

7.14 Extended evaluation of scattered light

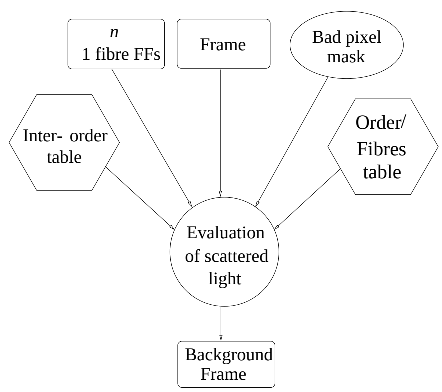

Figure 7.14: Evaluation of scattered light

Purpose:

Evaluation of the scattered light in a frame, using the available inter-order intervals *and* a few pixels over the fibres, in the bluest part of the frames, with simultaneous optimal extraction of the spectra *only in those few pixels*

Used in:

- step 3.8 (optimal extraction)
- step 4.4 (optimal extraction)

Inputs:

1. the frame whose background is to be evaluated
2. the Full Slit Flat Field frame
3. n single fibre Flat Field frames
4. Orders/fibres table
5. Inter order table
6. bad pixels mask

Outputs:

1. a frame containing the estimated background

Description:

As described in the document (see section 5.7.1), for any given x coordinate in a frame to be reduced the ADUs can be represented as a linear combination of the appropriate orders of the single fibre Flat Field frames plus a smooth (polynomial) background. A linear least squares fit is performed on all the available inter-order intervals and a few (not more than five) vertical segments covering the bluest, overlapping orders where there is no inter-order space left. Known bad pixels are not included in the fit. In this case, the background is expressed as

$$B(x,y) = \sum_{i,j} a_{ij} x^i y^j \tag{7.6}$$

and the χ^2 is expressed as the sum of two terms:

$$\chi^2 = \chi_1^2 + \chi_2^2, \tag{7.7}$$

where

$$\chi_1^2 = \sum_{(x,y)\in \mathbf{I}} M(x,y) \frac{(S(x,y) - B(x,y))^2}{V(x,y)} \tag{7.8}$$

and

$$\chi_2^2 = \sum_{x\in \mathbf{D}} \sum_{i=i_{\mathrm{low}}(x)}^{i_{\mathrm{upp}}(x)} M(x,y) \frac{\left(\frac{S(x,y)}{\mathrm{F}_{\mathrm{slit}}(x,y)} - \frac{B(x,y)}{\mathrm{F}_{\mathrm{slit}}(x,y)} - \sum_{n,m} c_n(x,m)\mathrm{F}''_n(x,y,m)\right)^2}{V(x,y)}, \tag{7.9}$$

where $\mathbf{D}$ is the set of x positions included in the vertical segments being used for the background estimation, the index n runs on the number of fibres present and the index m runs on the overlapping bluest orders to be considered simultaneously. The Science frame $\mathrm{S}(x,y)$ in these equations is bias and dark subtracted, but has not yet been divided by the Full Slit Flat Field frame $\mathrm{F}_{\mathrm{slit}}(x,y)$, as inter-order regions are used, and the division is expressed explicitly in the equations, where needed. The only differences between this equation and equation 5.7 in section 5.7.1 are the following:

- in this fit, both the spectra and the parameters of the smooth surface representing the background are varied simultaneously;
- the spectra at different x positions do not decouple in separate fits, due to the cross terms coming from the background.

It follows that the solution of this linear fit implies the inversion of a $\sim 200 \times 200$ matrix (relatively slow, but this does not loop over pixels and orders, it is done once for each background estimation). Then σ-clipping will be applied and the fit iterated until there are no new rejections. This will be implemented in a new C module of MIDAS, and will make use of some numerical library for the matrix inversion (endorsed by **ESO**, TBD).

7.15 Optimal extraction

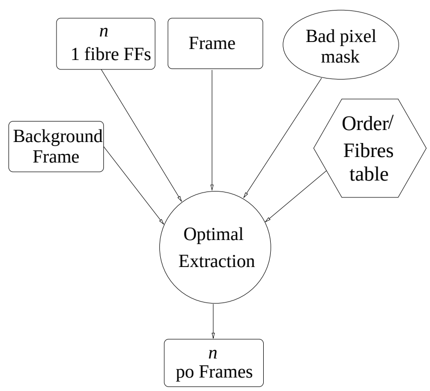

Figure 7.15: Optimal Extraction

Purpose:

Optimal extraction of the spectra from the n fibres with deblending and cosmic ray hits rejection

Used in:

- step 3.10 (optimal extraction)
- step 4.6 (optimal extraction)

Inputs:

1. Science or calibration frame from which the spectra are to be extracted
2. background frame

3. n single fibre Flat Field frames
4. Orders/fibres table
5. bad pixels mask

Outputs:

1. n frames containing the extracted spectra (pixel-order space)

Description:

As described in the document (see section 5.7.1), for any given x coordinate in a frame to be reduced the ADUs can be represented as a linear combination of the appropriate orders of the single fibre Flat Field frames plus a smooth (polynomial) background. For every x, separately for non overlapping groups of orders, a linear least squares fit is performed on the relevant portion of the frame. Known bad pixels are not included in the fit. In this fit, only the spectra are varied, while the background, previously determined, is held fixed. This implies the inversion of an $\sim 8 \times 8$ matrix for every x of every non overlapping order, and possibly a $\sim 32 \times 32$ matrix for the group of overlapping, bluest orders. Then σ-clipping is applied, variances recomputed and the fit iterated until there are no new rejections. This will be implemented in a new C module of MIDAS, and will make use of some numerical library for the matrix inversion (! endorsed by **ESO**, TBD).

7.16 Determination of the dispersion relations

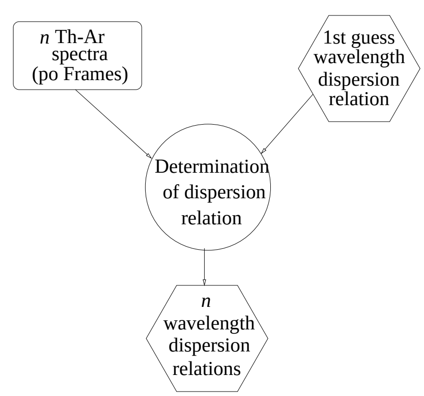

Figure 7.16: Determination of the dispersion relations

Purpose:

Compute coefficients of the wavelength dispersion relations

Used in:

- step 5.1

Inputs:

1. n reduced Th-Ar spectra in pixel-order space, one for each fibre
2. 1st guess preliminary wavelength dispersion relation

Outputs:

1. n tables, one for each fibre, containing line identifications, plus the parameters of the relevant dispersion relation, stored in keywords

Description:

Format check operation produces a raw approximation for the wavelength dispersion relation, bypassing any interactive line identification. This step, one fibre at a time, is identical to ordinary wavelength calibration in UVES in slit mode, and will therefore be performed by existing MIDAS procedures, simply looping over fibres. This will require a trivial MIDAS wrapper procedure to be implemented.

7.17 Higher order correction of the dispersion relations with simultaneous calibration

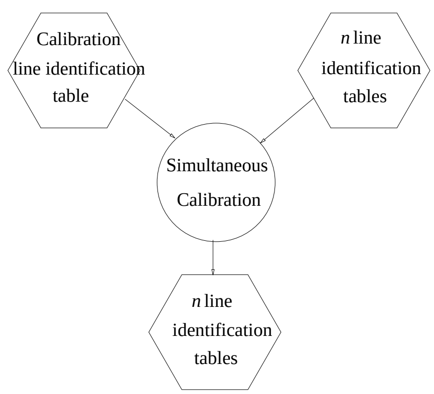

Figure 7.17: Higher order correction simultaneous calibration

Purpose:

Compute corrections to the coefficients of the wavelength dispersion relations using the spectrum of the simultaneous calibration fibre

Used in:

- step 5.2

Inputs:

1. n tables, one for each fibre in the Th-Ar calibration frame, containing line identifications, plus the parameters of the relevant dispersion relation stored in keywords
2. the table containing line identifications, plus the parameters of the relevant dispersion relation stored in keywords, derived from the simultaneous calibration fibre of a science frame

Outputs:

1. n tables, one for each fibre, containing line identifications, plus the *corrected* parameters of the relevant dispersion relation stored in keywords

Description:

Since (in simultaneous calibration mode) the simultaneous calibration spectrum is present both in the Th-Ar frame and in each Science frame, we get, from the wavelength calibration step, a dispersion relation (a) from that fibre in the Th-Ar frame and another dispersion relation (b) from that same fibre in each Science frame. Their difference yields a wavelength dependent correction that has to be applied to all the dispersion relations derived from the Th-Ar frame. Since the dispersion relations are in a polynomial form, this correction can be most simply applied as an additive correction to each of the coefficients, the correction being just the difference between the corresponding coefficients of (b) and those of (a).

This is a trivial task, and it may be easily implemented with a few MIDAS commands.

7.18 Rebinning of spectra

Purpose:

Moving a spectrum from pixel to wavelength space

Used in:

- step 5.3

Inputs:

1. n Science spectra in pixel-order space
2. n wavelength dispersion relations

Outputs:

1. n Science spectra in wavelength-order space

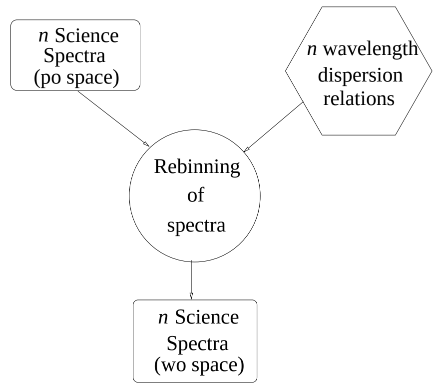

Figure 7.18: Rebinning of the spectra

Description:

A rebinning procedure is used upon spectra which have been extracted making use of a standard or optimal procedure. A separate pixel to wavelength dispersion relation is used for each fibre. Available MIDAS procedures can be applied without modifications, implementing a MIDAS procedure that loops over the whole set of fibres.

7.19 Sky subtraction from a Science spectrum

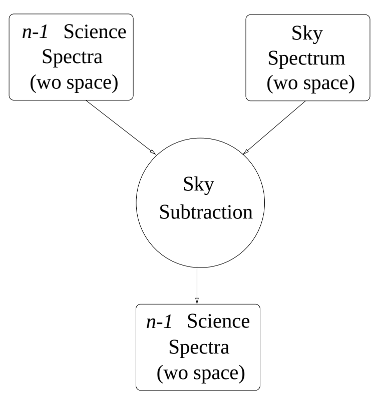

Figure 7.19: Subtraction of the sky spectrum

Purpose:

Removal of the sky flux contribution from extracted spectra

Used in:

- step 6.1

Inputs:

1. $n-1$ Rebinned Science spectra in wavelength-order space
2. Sky spectrum in wavelength-order space

Outputs:

1. $n-1$ Science spectra cleaned from sky flux contribution

Description:

If the astronomer chose to devote a fibre to the measurement of the sky flux, this spectrum has been extracted along with the remaining $n-1$ science spectra. All extraction schemes produce spectra corrected for different fibre throughputs and flat field, therefore (unless vignetting is selectively present on some of the fibres) the extracted sky spectrum can be plainly subtracted as it is from science spectra. A simple MIDAS procedure will recognise the sky spectrum (if present) from a descriptor and subtract it from the other $n-1$ frames of the set.

7.20 Order merging

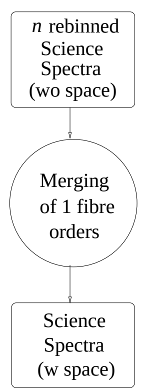

Figure 7.20: Merging of the orders in the spectrum of each fibre

Purpose:

To obtain a 1D spectrum for each fibre

Used in:

- step 7.1

Inputs:

1. n Rebinned Science spectra

Outputs:

1. $n-1$ (or n, if no fibre was devoted to the sky) final 1D Science spectra in wavelength space

Description:

This step, one fibre at a time, is identical to ordinary order merging for UVES in slit mode, and will therefore be performed by existing MIDAS procedures, simply looping over fibres. This will require a trivial MIDAS wrapper procedure to be implemented.

8 Results from numerical experiments on UVES test frames

Numerical experiments have been performed, to test prototype data reduction procedures conceptually similar to those described in this document. They are used to assess the feasibility of the chosen methodological approaches, and the requirements for their applicability.

We have run sets of simulations of fibre-fed echelle spectra of plausible astronomical targets (continua with varying slopes, plus absorption/emission lines), with the following characteristics:

- Simulated flat-field and science frames of size 1024×1024 pixels
- Pixel-to-pixel variations (random ±10%)
- Hot pixels, at fixed and known positions (saturating the CCD)
- Approximate blaze function (quadratically decaying from image centre)
- A flat, uniform across the detector, scattered light component
- Eight fibres, with transmission variable from fibre to fibre
- Fibre cross-dispersion profile as derived from fibre-fed UVES test data (gaussian convolved with rectangular Π function)
- Spectral line profile along dispersion is gaussian
- Order positions and slopes following the echelle rule
- Poisson noise included in both flat-field and science simulated frames
- Cosmic ray events added to science frame, with all possible intensities up to saturation (10000 events, 1-2 pixels long)

The simulator includes selectable parameters, that were set at the following values:

- bluest (highest) order $m_0 = 102$

- starting y coordinate of order m_0 = 90. pix
- starting separation between bluest orders = 81. pix
- slope of order m_0 = 0.02807617
- number of fibres = 8
- width σ of gaussian component of fibre profile = 1.9 pix (*from test data*)
- width of Π-function component of fibre profile = 0.9 pix (*from test data*)
- inter-fibre spacing = 10.0 pix (*from test data*)
- coefficient of quadratic term of the blaze function = 2.e-6
- scattered light = 100. counts/pix
- CCD saturation value = 1.e5 counts
- spectra line width (gaussian σ) = 1.0 pix
- fractional deviation from linearity of CCD below saturation = 0.0

Then we have proceeded as follows:

- A prototype of our optimal-extraction algorithm, outlined in section 4.3.1, has then been run on these simulated data, to extract the spectra belonging to individual fibres. Particular attention was paid to obtain a good deconvolution between adjacent fibres; no provision has been however made (yet) for neighbouring interfering orders in the blue. Also the effective rejection of cosmic rays was carefully checked. During the reduction, quality controls such as χ^2 and rejected pixel fractions (both order-by-order and overall) are printed out.
- Next, the same reduction method was applied to simulated data where a small shift was introduced, relative to the flat-field frame used in the extraction. These shifts are in the range 0.05-0.45 pixels, sampled in steps of 0.05 pixels.
- Both previous steps (i.e. with and without shifts between flat-fields and science data) have been repeated for simulated targets of different SNRs. One simulation was made with all targets having low ($\sim$ 20) SNR (per pixel), a second one with all targets having medium-high ($\sim$ 70) SNR, and a third one with all targets having very high ($\sim$ 200) SNR. Finally, a further simulation was made with targets spanning the whole SNR range from 20 to 200, distributed among the 8 fibres. This last test was made to test the extraction in the worst case of fibre cross-contamination, namely a source with SNR $\sim$ 200 polluting a much weaker neighbouring source with SNR $\sim$ 20.

- Last, we have investigated the effect of a broadening of the fibre image in the science frame with respect to the flat-fields (possibly arising from jitter during the exposure), yielding a slight mismatch between the cross-dispersion PSF of science and flat-fields frames, respectively. We have made such tests using, as input, spectra of mixed-SNR targets. The test has been repeated for a broadening with a rectangular profile of various widths (from 0.2 to 2.0 pixels), and with a double-peaked profile (peak separation 0.6 pixels).

The results have been examined both visually, and with reference to the χ^2 statistics and rejected pixel fraction, resulting from the fitting. The detailed results are different for different SNRs of the targets, and we describe them now:

- **Case of low SNR:**

  1. *No shift:* In this case, the main factor limiting accuracy is photon statistics. In spite of that, the results are satisfactory. Cosmic ray hits are rejected efficiently by optimal extraction: at most a dozen, mainly low-level events (out of 10000) are still visible in the reduced spectra. We obtain an overall reduced $\chi^2 \sim 0.68$, and visual inspection of the reduced spectra does not show appreciable cross-contamination between adjacent fibres (Figure 8.1). The fraction of rejected pixels is around 2%, except in the bluest orders where cross-order contamination (not dealt with still) is severe.
  2. *With shift:* Since the dominant source of error here is photon statistics, the reduction is not very sensitive to the *systematic* error introduced by a shift between flat-fields and science data. In particular, if we define $\Delta\chi^2 = \chi^2(shift) - \chi^2(shift = 0)$, we obtain a $\Delta\chi^2 = 1$ for a shift of 0.35 pixels. This is the practical applicability limit for our optimal extraction procedure, in the case of low SNR spectra.

- **Case of medium-high SNR:**

  1. *No shift:* In this case the photon statistics is high enough to allow a much more accurate spectrum extraction. For comparison, we show in Figure 8.2 the same spectral range as in Figure 8.1 (with the same input spectra). Cosmic ray hit rejection is also better, with only a couple residual un-rejected events out of 10000. With this photon statistics, systematic errors come into play: while this is not the case for inter-fibre cross-contamination, which is effectively corrected, as shown, it is instead the case for cross-order contamination in the blue (see Figure 8.3, fibre #8). This correction will be included in the final reduction program. Figure 8.3 shows the impact of a missing de-contamination: for fibre #8 absorption-line equivalent widths are significantly reduced, and the continuum misplaced (compare with Figure 8.2, where cross-fibre corrections are applied, and cross-order contamination is zero: here all equivalent widths may be measured reliably and the continuum level oscillates around its true value).
  2. *With shift:* For medium-high SNR spectra, the reduction is fairly sensitive to the systematic error introduced by a shift. We now obtain a $\Delta\chi^2 = 1$ for a shift of 0.15 pixels. To visualise the degradation in the reduced spectra as this shift increases from 0.0 to 0.3 pixels, we report

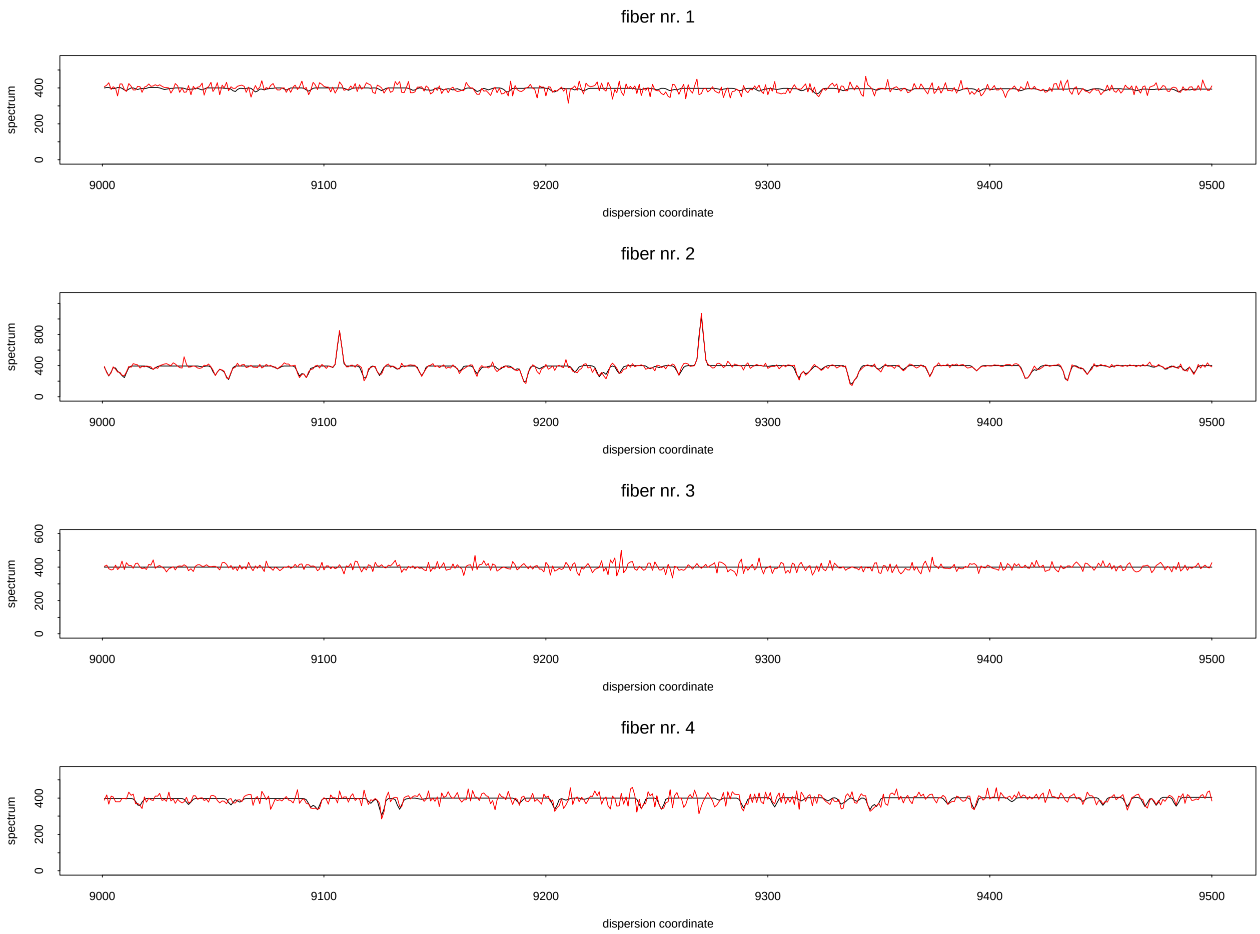

Figure 8.1: Example of low-SNR spectra, reduced using optimal extraction with fibre deconvolution (only fibres 1-4 are shown). Input spectra are plotted in black, reduced spectra in red (or gray for B/W printers). The deconvolution works well, despite the evident low SNR, as evidenced by e.g. the intense emission lines in fibre #2, that are completely rejected from the reduced spectra of neighbouring fibres #1 and #3.

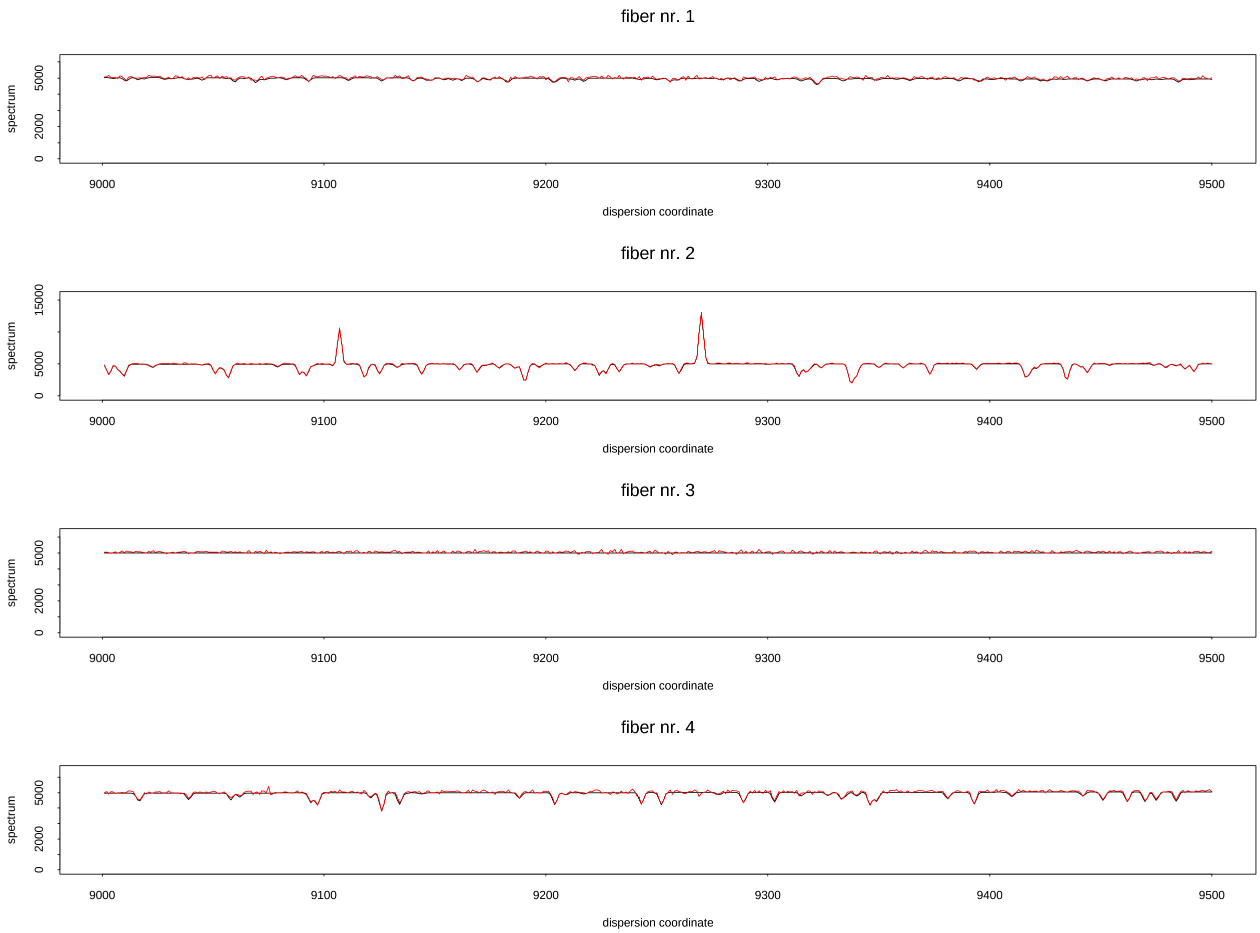

Figure 8.2: Medium-high-SNR spectra, reduced using optimal extraction with fibre deconvolution (only fibres 1-4 are shown). The spectral range is the same as in Figure 8.1.

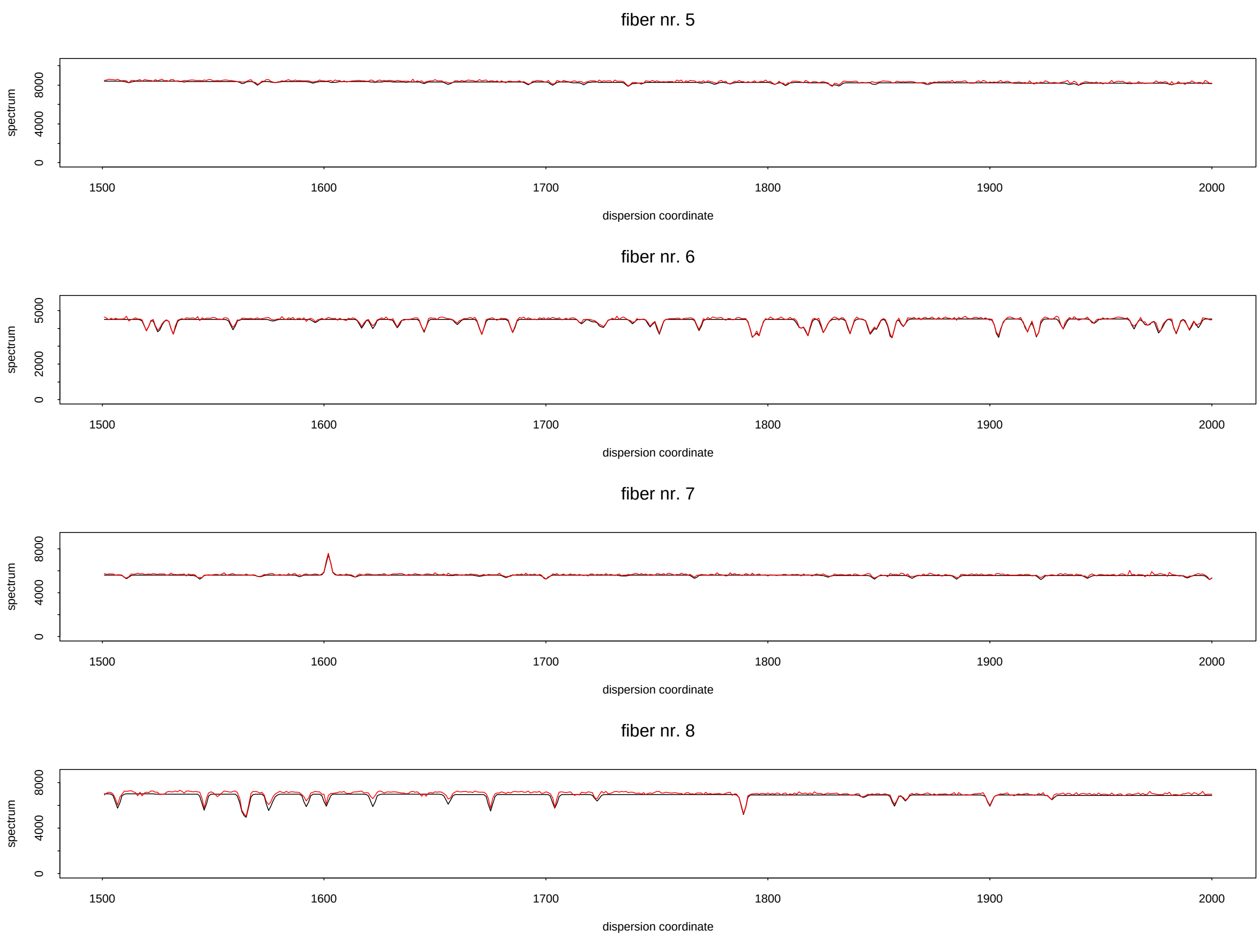

Figure 8.3: Medium-high-SNR spectra, with fibre deconvolution *but no cross-order deconvolution*, showing the effect of a missing deconvolution on the reduced spectra (especially fibre #8, contaminated by fibre #1 of the neighbouring order).

in Figure 8.4 a small section of the extracted spectrum for a single fibre (after deconvolution): it is clear that while a shift up to 0.2 pixels is still tolerable (at least visually: the χ^2 may give a more stringent constraint), a shift of 0.3 pixels produces an unacceptably noisy extracted spectrum, including pixels where the fit converges at totally wrong values. This shows that whenever $\Delta\chi^2 = 1$ is significantly exceeded, the results are very unlikely to be acceptable.

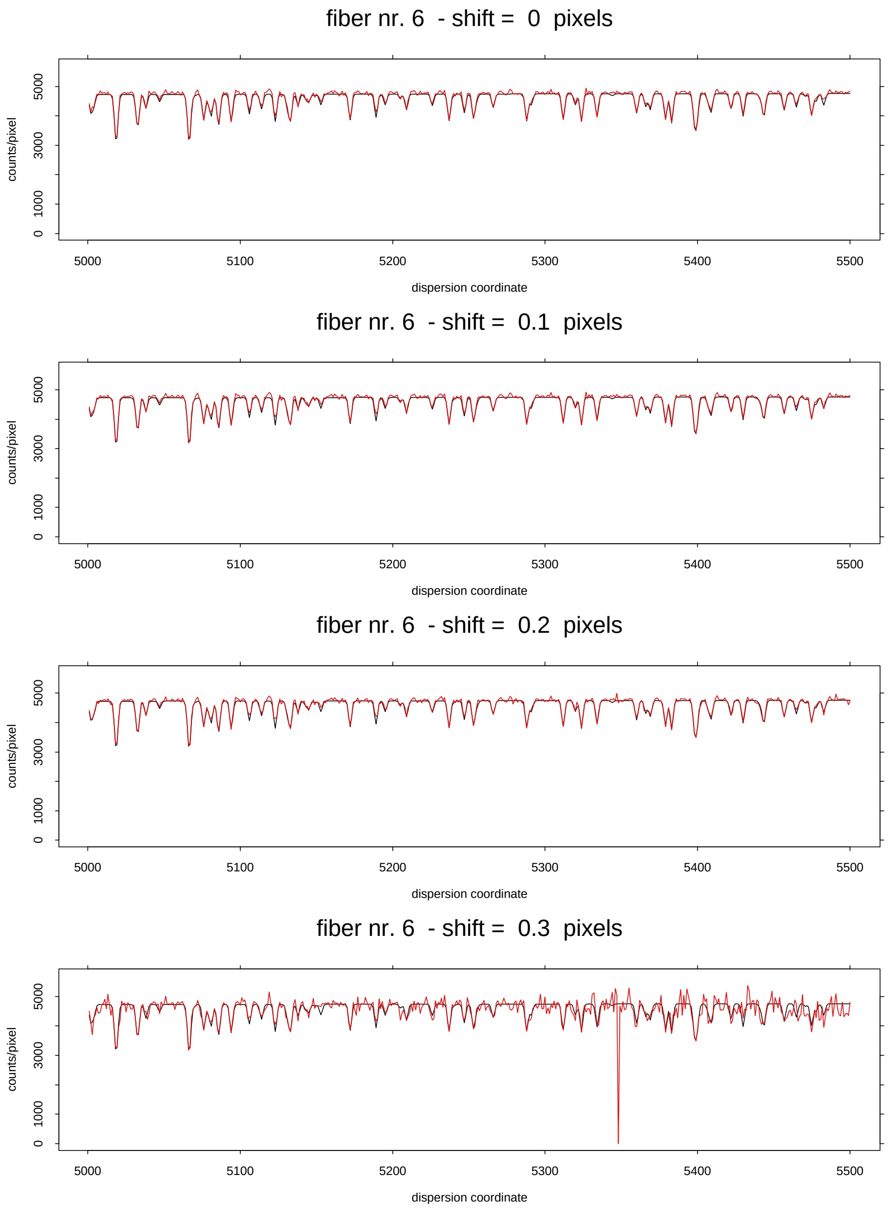

Figure 8.4: Example of reduced medium-high-SNR spectra, with a variable amount of shift between flat-field and science data, as indicated.

- **Case of very high SNR:**

  1. *No shift:* The best that can be obtained. Cosmic ray rejection is virtually 100%. Statistical errors are irrelevant, and fibre deconvolution very accurate (Figure 8.5, in the same spectral range as before). Accordingly, systematic errors are exacerbated, and a missing (for the time being) blue cross-order deconvolution becomes critical (Figure 8.6, fibre #8).
  2. *With shift:* Since systematic errors are now extremely important, even a very small shift is now critical, In fact, we meet the $\Delta\chi^2 = 1$ condition already for a shift of 0.05 pixels ! While this is a very stringent constraint, and may easily imply that new calibrations are to be taken for each science exposure, having all fibres fed with very high SNR spectra will probably be a rare occurrence. Therefore, such tight constraints will only rarely apply in practice.

- **Case of mixed high and low SNR:**

  1. *No shift:* This case was checked in order to ensure that fibre deconvolution works even in the most unfavourable condition where one high-SNR object and one low-SNR object are placed in neighbouring fibres. Our test shows that it indeed works: as an extreme example, an object with a continuum level of $\sim$ 800 counts/pixel is placed in fibre #6, next to a brighter object with continuum of $\sim$ 50000 counts/pixel in fibre #7, but the extracted (deconvolved) spectrum of the weaker one is entirely unaffected by the stronger one (Figure 8.7). The average continuum level of the weak object is recovered correctly, and a bright emission line of the stronger object has no visible effect on the reduced spectrum of the weaker object.
  2. *With shift:* The sensitivity to shift in this mixed case is not easily described by a simple $\Delta\chi^2$ condition. This is dominated entirely by the presence of the strongest objects (most sensitive to systematic errors), and the applicability limit for $\Delta\chi^2 = 1$ may by as narrow as a maximum shift of 0.05-0.1 pixels. However, for most of the fibres the reduction accuracy will be still good for larger shifts (0.1-0.2 pixels). The ultimate applicability range will therefore depend on the user choice, according to the priorities he/she assigns to individual targets.

To summarise, we plot in Figure 8.8 the values of pixel shifts that are acceptable, in order not to exceed $\Delta\chi^2 = 1$, for different SNR values. Before tests can be applied to real commissioning data, with final fibres, this Figure may be used to estimate the expected limits of applicability of our optimal extraction procedure, allowing the user to take a decision when these conditions are not met, already before a complete reduction is performed.

- **Case of mixed high and low SNR, plus broadening:**

  1. *Rectangular broadening:* The simulated science frames (each including targets with SNR in the full 20-200 range) have been convolved with a broadening function, rectangular with various widths, to simulate different amounts of jitter during the science exposure. The flat-field frames have instead not been convolved, since the expected jitter during a flat-field exposure is expected to be negligible. We have then applied the reduction using together convolved science frame and un-convolved flat-fields, and we have evaluated the goodness of the output reduced

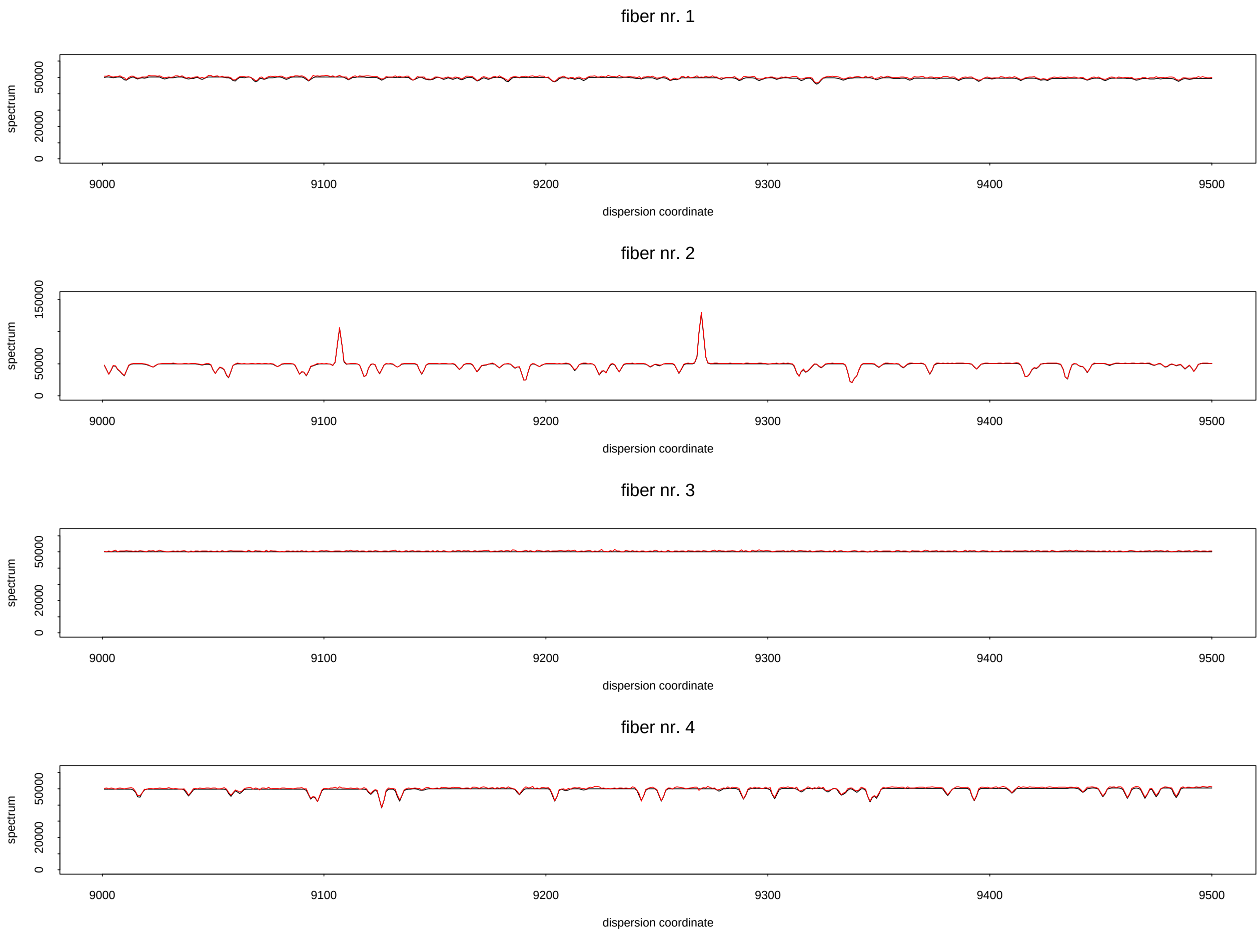

Figure 8.5: High-SNR spectra, reduced using optimal extraction with fibre deconvolution (only fibres 1-4 are shown). The spectral range is the same as in Figure 8.1.

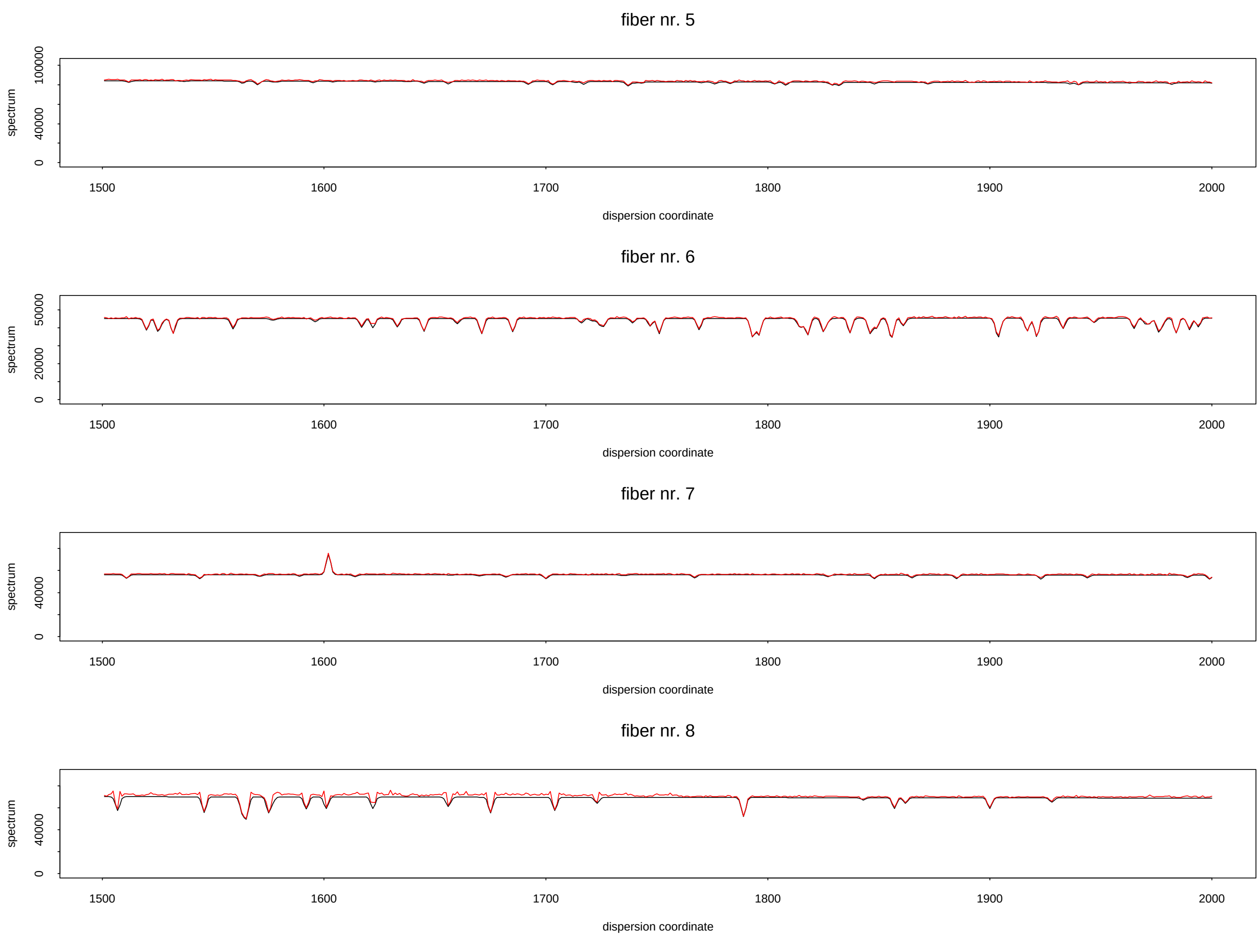

Figure 8.6: High-SNR spectra, with fibre deconvolution *but no cross-order deconvolution*, showing the effect of a missing deconvolution on the reduced spectra (especially fibre #8, contaminated by fibre #1 of the neighbouring order).

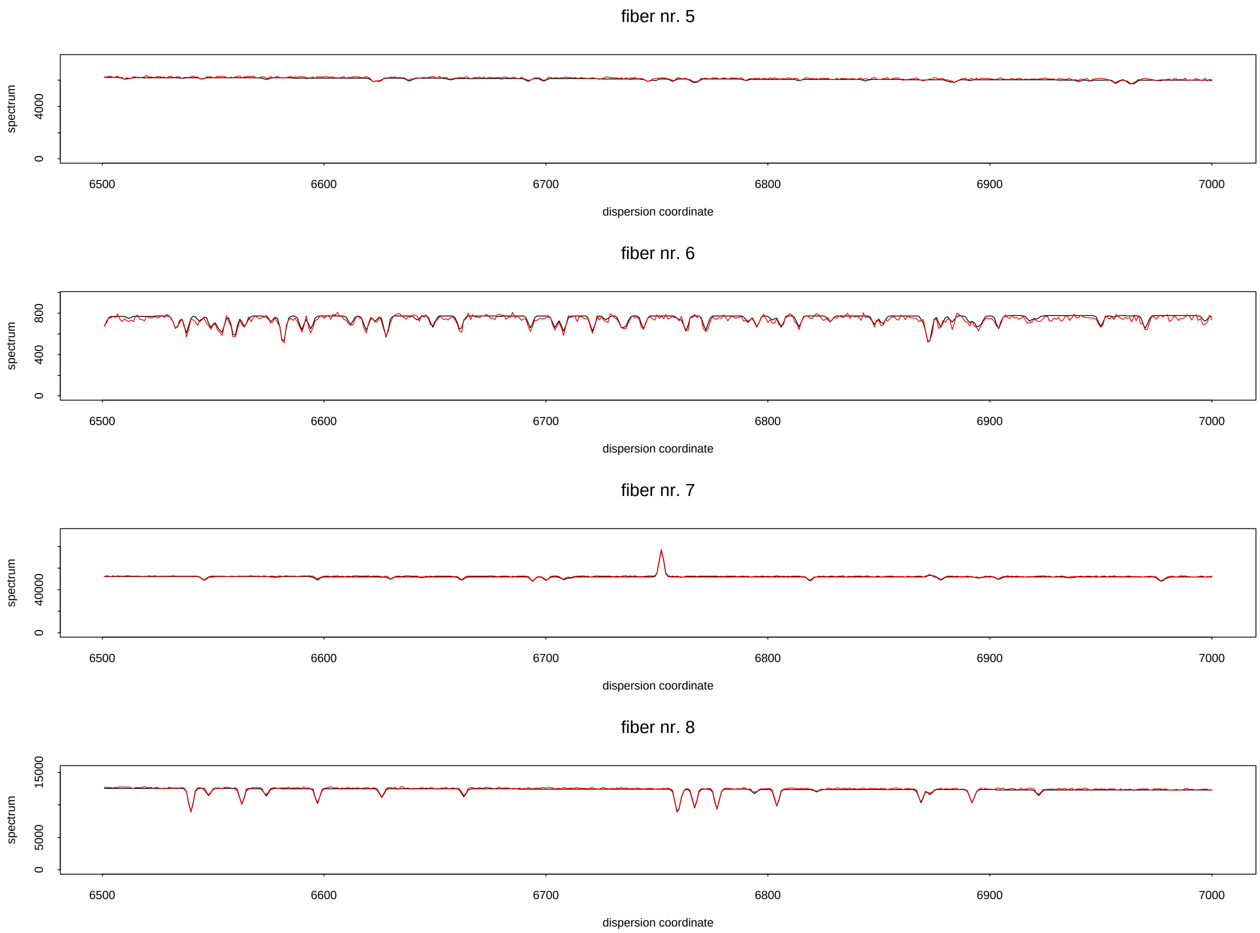

Figure 8.7: Mixed-SNR extracted spectra, with fibre deconvolution, showing the effectiveness of the deconvolution on the spectra of objects with very different SNRs (see fibres #6 and #7).

spectra, both in terms of overall χ^2 and rejected pixel fractions, and by visual inspection of the reduced spectra themselves. As a result, broadening widths in the range 0.2-0.5 pixels have an entirely negligible impact on the final reduced spectra, for any SNR level, both using χ^2 and direct inspection; on the contrary, a broadening of 2.0 pixels causes a noticeable increase in χ^2 ($\Delta\chi^2 > 1$) and sensibly inaccurate output spectra; the case of 1.0 pixel broadening is the borderline case, with χ^2 and output spectra still acceptable. Inaccuracies are most visible as systematic errors in the highest SNR spectra (SNR$\sim$200), and at most at a level of very few percent (2-3%); it is worth noticing that the fit converges everywhere, and no "crazy" values are output in any part of the reduced spectra. Therefore, a broadening of 1.0 pixels for the fibre images in the science frames can be considered as the acceptability limit for our reduction method.

2. *Double-peaked broadening:* We have also checked that, if the broadening is not a rectangular function (namely, uniform probability within two extremes), the acceptability threshold does not vary much. As the opposite extreme, we have taken a broadening function made of two very narrow peaks, spaced 0.6 pixels apart. After reduction of the science frames simulated in this way, we obtain indeed results that are as acceptable as the 1.0 pixels uniform broadening. Therefore, also in this case tolerance to broadening effects is not dramatically different from the uniform broadening case.

Summarizing, the effect of a broadening, caused by jitter during a science exposure, is far less critical for our method than the effect of an overall shift across dispersion. Tolerances are far more relaxed, and if such a broadening does not exceed 0.6-1.0 pixels, whatever its detailed distribution is, its impact on the quality of the output spectra can be considered negligible, even if no correction at all is applied to compensate it.

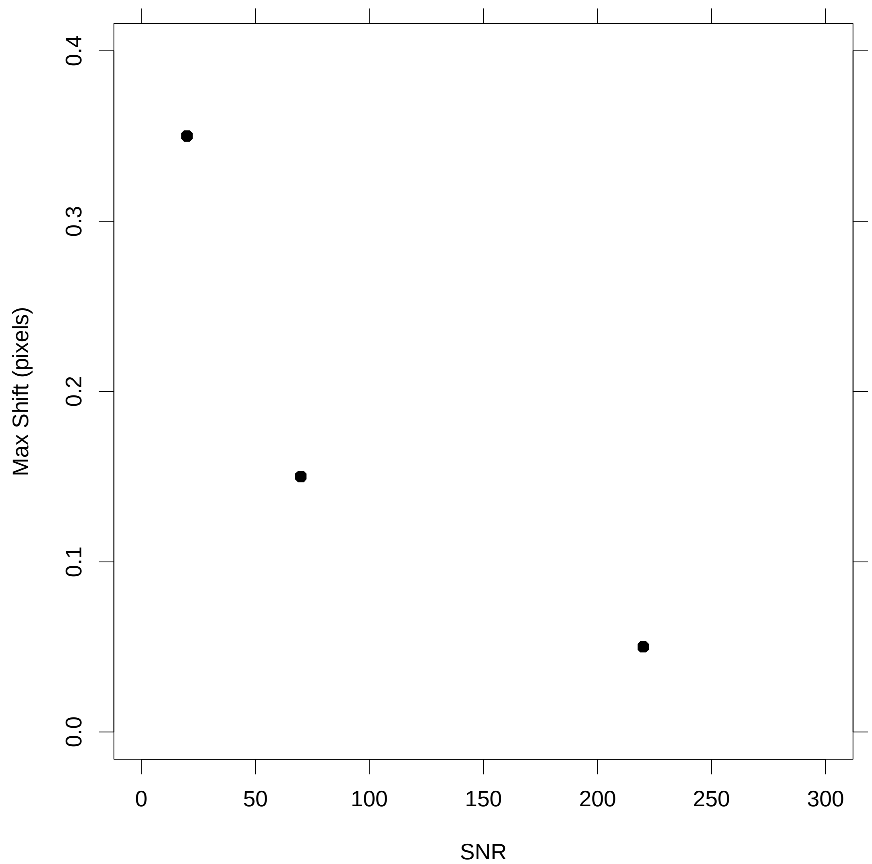

Figure 8.8: plot of maximum acceptable shifts between flat-fields and science data, as a function of the SNR of the target objects.